

DESIGN AND IMPLEMENTAION OF A NET-ZERO MOBILE RESIDENCE WITH  
PREDICTIVE CONTROL

A Project Presented to  
The Faculty of the Department of Mechanical Engineering  
San Jose State University

In Partial Fulfillment  
Of the Requirements for the Degree  
Master of Science

by  
Keith Christman  
May 2018

© 2017

Keith Christman

ALL RIGHTS RESERVED

The Undersigned Committee Approves

DESIGN AND IMPLEMENTAION OF A NET-ZERO MOBILE RESIDENCE WITH  
PREDICTIVE CONTROL

by

Keith Christman

APPROVED FOR THE DEPARTMENT OF MECHANICAL ENGINEERING

---

Dr. Saeid Bashash, Ph.D, Committee Chair Date

---

Dr. Mohamed Badawy, Ph.D, Committee Member Date

---

Dr. Burford J. Furman, Ph.D, Committee Member Date

## ABSTRACT

### DESIGN AND IMPLEMENTATION OF A NET-ZERO MOBILE RESIDENCE WITH PREDICTIVE CONTROL

by Keith Christman

Renewable sources of energy can be applied to residential or commercial buildings with the goal of generating the entirety of power consumed. The net value of consumption minus generation in an ideal design would equal zero which encompasses the nomenclature given to these residences as net zero. The construction and fabrication necessary for a net zero environment is applied to a mobile residence accompanied by a theoretical model of the system. The theoretical model consists of an empirically derived thermal model for the mobile residence as well as an electrical model based on the components used in the constructed mobile residence. Predictive temperature control was then implemented based on forecasted temperature and UV index data to aid the user in choosing an internal set point temperature while preventing the undesirable excessive discharge of the battery bank.

## ACKNOWLEDGEMENTS

The interest and involvement of my committee members has first and foremost made this project possible. Personally, I would like to thank Dr. Saeid Bashash for initially sparking the interest in this field and tirelessly providing needed feedback and encouragement along the way. Dr. Mohamed Badawy for shedding light on key electrical concerns and providing an academic foundation in an area that is not my strongest knowledge base. Many of his insights guided the project in a positive direction. And Dr. Burford J. Furman for investing his time and interest in the topic also for guiding me to publish content for fellow engineers interested in the same undertaking.

## TABLE OF CONTENTS

ABSTRACT.....	4
ACKNOWLEDGEMENTS.....	5
TABLE OF CONTENTS.....	6
NOMENCLATURE.....	7
LIST OF TABLES.....	8
LIST OF FIGURES.....	9
1.0 INTRODUCTION.....	10
1.1 Literature Review.....	12
1.2 Objective.....	12
2.0 METHODOLOGY.....	12
2.1 Analytical Work.....	12
2.2 Fabrication.....	18
2.3 Thermal Model.....	24
2.4 API to Wunderground.....	28
2.5 UV index to Solar Irradiance.....	28
3.0 RESULTS AND DISCUSSION.....	33
3.1 Predictive Model with Intelligence.....	33
3.2 Temperature Extremes.....	34
4.0 CONCLUSIONS AND FUTURE WORK.....	36
REFERENCES.....	37
APPENDIX A. MATLAB CODE.....	38
APPENDIX B. API MATLAB CODE.....	41

## NOMENCLATURE

SOC – State of Charge

LTC– Linear Technologies Chip

## LIST OF TABLES

Table 1-Battery Bank and Solar Capacity.....	12
Table 2-Energy Consumption Estimate.....	13
Table 3- Inductor sizing calculations.....	14
Table 4-Input capacitor sizing calculations.....	14
Table 5-Output capacitor sizing calculations.....	14
Table 6-Mosfet sizing calculations.....	15
Table 7-Electrical components housed.....	23
Table 8-Tabulated solar irradiance to current relationships.....	30

## LIST OF FIGURES

Figure 1- LTC4015 Eagle circuit schematic.....	15
Figure 2- LTC4281 Eagle circuit schematic.....	16
Figure 3- LT8390 Eagle circuit schematic.....	17
Figure 4- PCB Eagle board Layer 1.....	17
Figure 5- Manufactured PCB with IC's soldered on.....	17
Figure 6- Populated PCB board.....	17
Figure 7- Fabricated and populated electrical containment box.....	18
Figure 8- Electrical containment box framing.....	18
Figure 9- Electrical containment box populated with large components.....	18
Figure 10- Electrical containment box drawing for fabrication.....	19
Figure 11- Solar panel frame CAD model.....	19
Figure 12- Solar frame CAD assembly.....	20
Figure 13- Front frame mid welding operation.....	20
Figure 14- Rear frame mid welding operation.....	21
Figure 15- Solar wiring.....	21
Figure 16- Solar Mounting.....	22
Figure 17- App home screen for Victron MPPT 100/30.....	22
Figure 18- Electrical components in electrical containment box.....	23
Figure 19- Thermal data acquisition tool.....	24
Figure 20- First order internal temperature approximation and actual internal temperature data.....	25
Figure 21- Saturated sunlight data.....	26
Figure 22- Second order internal temperature approximation and actual internal temperature data.....	27
Figure 23- Saturated sunlight data and UV index data.....	27
Figure 24- Second order internal temperature approximation from UV data and actual internal temperature data.....	28
Figure 25- API code.....	28
Figure 26- UV index data.....	29
Figure 27- UV index data to Solar Irradiance.....	29
Figure 28- Solar Irradiance to Isolar relationship.....	30
Figure 29- Manufacture publish I-V curves.....	30
Figure 30- Simplified electrical model.....	31
Figure 31- Switch states logic.....	32

## 1.0 Introduction

There has been a conscious shift focusing on the negative externalities due to non-renewable energy generation. Global warming, pollution, and climate change are detrimental side effects to the current energy dependency [1]. The global new investment in renewable power and fuels grew from 39.5 billion (USD) in 2004 to 270.2 billion in 2014 [1]. Solar energy is at the forefront of the energy revolution bolstering key benefits such as no practical emissions of CO<sub>2</sub> during operation, and no dependency on consumable energy imports such coal or natural gas [1]. Solar energy as a renewable energy source has been a motivating addition to current grid connected energy systems, or micro-grids. Unlike micro-grids, which are ultimately grid dependent, in a net zero energy system the quantity of energy consumed is equal to the quantity generated. A dependency on grid power is no longer necessary, defining flexibility and autonomy from the current energy landscape. After the initial investment for a system is made energy generation cost is no longer a periodic burden. A commitment to non-polluting renewable energy is made. And in the case of a mobile vehicle platform the modern amenities are available and no longer depend on location. It is argued that energy demand will only increase in the future due to economic growth, developing countries and population increase [2]. To complement renewable energy users also need to understand their consumption habits and the magnitude of energy that they consume. There are current economic motivations to decrease energy consumption but an understanding of how certain actions overall effect total consumption is limited to the modern consumer. When an energy user decides to turn off a computer or a light, the understanding of how much power that saves is generally lost. With a net zero energy system the user is intimately involved with his or her energy habits. Ultimately there is no power plant to supply a seemingly unlimited amount of power. Instead a user must understand how much energy his or her system can generate and conversely how much user habits will consume the available energy. The focus of the following discussion will be on energy impacts due to an air conditioning unit in a mobile residence. The set point temperature of the air conditioner largely dictates the amount of energy consumed. Presenting an intuitive and logical suggestion to the user for an ideal set point temperature is the goal.

### 1.1 Literature Review

Given the vast breadth of potential research topics for the proposed project the area of interest has been narrowed down to the following two topics. The first being the design and fabrication of a net zero energy system comprised of solar, battery bank and charge controller. The second is how to convey sensible energy consumption targets to the user via their own habits and desired internal temperature.

Ricardo Vidal Lorbada [12] presented a design and implementation of a solar array, lithium ion battery bank and charge controller in his master's thesis. The project highlighted the use of Linear Technologies readily available IC chips that focus on power management. The LTC4015 chip is marketed as a solar to battery charge controller. It enables MPPT on the solar side as well as constant current constant voltage charging profiles for multiple battery chemistries. The proposed system by Ricardo was insufficiently low in its power rating for the mobile system requirements, however the backbone of the system the LTC4015 chip could still be used. The implementation of the LTC4015 chip requires designing and specifying the adequate components for the given power requirements of the mobile platform. The use of data sheets published by Linear Technologies [13] made this possible. Supplemental reading explaining the necessity of components for buck converter design was provided by industry motivated application notes published by [9] Texas instruments and [8] Rohm. These documents give a fundamental understanding of the calculations required for sizing components in the power system

being implemented. Design tools such as EAGLE software to develop manufactureable PCB's was also mentioned in Ricardo's paper. Allowing complete customization of circuit design. Although comprehensive, Ricardo's thesis lacked a reoccurring theme in most energy storage systems for net zero residential buildings. A way to consistently control the voltage delivered to the expected system loads. The majority of systems use converters: boost, buck or buck-boost depending on the specific voltage constraints of the system. As discussed in papers by Filomeno M. Vieira and Shunlong Xiao [10, 11] the reliance on batteries as a means of energy storage deems necessary the use of converters on the battery output to maintain a consistent and predicable voltage supply. The authors reiterate that batteries are a fundamental piece to the net zero equation to smooth the unpredictability of solar generation and user consumption. The inherit voltage range that a battery can supply depending on its state of charge needs to be controlled. A DC-DC converter in between the battery and DC bus ensures the load voltage is consistent.

A net energy building revolution can in part be fueled by federal incentives and competitions, an example being the solar decathlon held by the U.S. Department of Energy. Of particular interest was the house designed and built by the University of Illinois [4, 5]. The energy generation of the net zero home was completely solar. An emphasis was placed on efficiency and even though the solar array's total surface area was smaller than the majority of other competitors it yielded a high net energy output because of its energy monitoring and control. The net energy consumption and generation was published to the user, citing it as a key aspect to the system. The readily available net energy information, as the paper stated "encouraged conservation". The user was also given control of their energy habits. The system used on/off lighting control, door and window monitoring, and HVAC set point control. All of which was easily accessible and manipulated via a clean user interface on an iPad. Understandably these professional touches were part of the 2011 home entered in the competition, while the 2009 home offered an insight to the initial proof of concept technologies that were polished come 2011. The home presented by the University of Illinois inspires the practicality of using solar as the sole energy generation as well as empowering the user with energy knowledge to make efficient consumption decisions. The user is empowered to control the set point HVAC system and lighting. These details are also of interest for a mobile platform. However some deviation is required when applying a net zero blue print to a mobile platform. Window and door monitoring is less of a priority because the living square footage is much smaller in a mobile platform that the user would be responsible for recognizing the inefficiencies associated with leaving a window or vent open.

Having raw energy generation and consumption data can be beneficial, but some sources argue the importance is on how the data is conveyed. It is argued that the user interface and design dictates its end efficiency. Continued research done on the North House [6] (2009 Solar Decathlon) concentrate on the niche subject of how to convey the information effectively to the consumer. The Fraser design team [6] emphasizes that the visualization of energy should "support residents in decision making tasks that integrate with their patterns of everyday life". The energy monitoring tool should allow consumers to execute actions directly as well as understand how these actions affect their daily habits. These conclusions could be implemented in a mobile platform and should be used to bolster user interaction and thus efficiency. The main factors influencing the visualization of energy consumption according to G. Wood and M. Newbrough [7] are display location, display units and timescale while the studies done by the Fraser team [6] add social interaction, personal milestones and community involvement. In the context of a mobile platform personal milestones or achievements could be easily made a design priority for the visualization of energy data.

## 1.2 Objectives

The proposed project consists of the design, build out and implementation of a net zero energy system for a mobile residence. The functioning electrical and thermal system will be theoretically modeled. The model will enable consumption predictions to be made for the following 60 hours. Required forecast data for external temperature and UV index data will be accessed via an API. The model will aid the user in suggesting an ideal set point temperature based on the forecast and desired internal temperature all while respecting a SOC (state of charge) battery bank minimum threshold.

## 2.0 Methodology:

The first step in designing and net zero system is to evaluate or estimate energy consumption. The estimation determines the solar array, battery bank and power requirements of the charge controller. The following section details how these estimates were calculated and tabulated.

### 2.1 Analytical Work

#### Battery Bank Capacity

An efficient stand-alone system that has the means of operating when solar irradiance is zero or minimal needs an energy storage system. Lithium ion batteries have a high-energy density in comparison to competition. While currently still expensive compared to counter parts, trends in automakers and even homes using these batteries suggests that an understanding in this technology will be fruitful for future years [12].

The battery voltage was chosen was 12 volts because it is ideal for many readily available DC components because of the standard used in the auto industry.

Based on the expected components seen in Tab. 2 the system is calculated to consume 2730 Watt-hrs per day.

Assuming a 12 volt battery the Amp-hrs needed is 227.5 Amp-hrs. The calculation can be seen in Eq. 2.1.1 and tabulated in Tab. 1. It should be noted that energy consumption is based on one day of use with a 1.5 factor of safety applied to the final value, increasing the expected consumption.

$$(Amp \cdot hrs) = \frac{\left(\frac{Watt \cdot hrs}{day}\right)}{(Battery Voltage)} \quad (2.1.1)$$

#### Solar Array Capacity

Any stand-alone power system must contain the means to generate power. Solar was chosen because of the relative ease of mounting to a movable structure (van), long lifetime, and high energy return operating in California weather. Preliminary calculations were made to ensure the solar array can supply enough energy for intended use. Additional attention on the 500 Watt peak air conditioner was placed to makes sure the panels could supply equivalent power at the maximum power point of the panels. Table 2 sums the expected energy consumption. Assuming 6 hours of max power generation per day, 530 Watts would supply adequate power for the expected system. The mounting space available also

Battery Bank		
Battery Voltage	12	
Needed Battery Amp-hrs	227.5	
Solar Panels		
Solar Irradiance (W/m <sup>2</sup> )	1000	800
Vmpp (Volts)	31.3	28.5
Imp (Amps)	8.8	6.95
Watts	275.44	198.075
Quantity of Panels	2	2
Predicted Hours at Max Operatio	6	6
Energy per Day (Watt-hrs/day)	3305.28	2376.9

Table 1) Battery Bank and Solar Capacity

constrained the allowable dimensions of the panels therefore 2 solar panels each with a 275 Watt power rating will be used.

$$\frac{\text{Energy}}{\text{day}} \left( \frac{\text{Watt} \cdot \text{hrs}}{\text{day}} \right) = (\text{Watts}) \cdot (\text{Quantity of Panels}) \cdot \left( \frac{\text{Hours at Max Operation}}{\text{day}} \right) \quad (\text{Eq. 2})$$

Energy Consumption				
	Volts	Watts	Daily Run Time (hrs)	Watt-hrs/day
DC Loads				
Air Conditioning	12	500	1	500
Fridge (optional)	12	30	24	720
AC (Inverter) Loads				
Laptop Charging	110	100	2	200
Phone Charging	5	5	2	10
Flood Lights	110	300	0.5	150
Coffee maker	110	1200	0.2	240
Total *no F.S. (Watt-hrs/day)				1820
Consecutive Days no charge			1	
Factor of Safety (inefficiencies)			1.5	
Total per Day (Watt-hrs/day)				2730

Table 2) Energy Consumption Estimate

#### LTC4015 Circuit

The system requirements set a threshold for the charge controller. The LTC4015 can support a max voltage of 35V and 20 Amps, making it a satisfactory starting point. The goal of the LTC4015 circuit is to step down the voltage coming out of the solar panels to an appropriate battery charging current. The battery charging then follows the preprogrammed CC-CV profile. If the battery does not need charging the system line of the LTC4015 then supplies voltage and current to LT8390 which will be discussed later.

Key components of the LTC4015 circuit are sized accordingly to handle the expected current and voltage of the system. Below is a list of tabulated calculations that follow equations presented in the datasheet [13]. Switching frequency is established via a resistor at 500000 Hz. The sense resistors at the input and output dictate the allowable current on the input and output, while the maximum input voltage is controlled via a voltage divider.

The inductor which is an essential part of the buck converter is sized according to the datasheet [13]. Supplemental calculations are also made using a Power Electronics text book by Daniel Hart. The tabulated results are compared.

Inductor Calculations: LTC4015 Datasheet				
Inductor Calculations	H	$L_{\text{calculated}}$	2.12E-06 Claims inductor ripple will be 25% of $I_{\text{CHG(MAX)}}$	
	H	$L_{\text{spec'd}}$	4.70E-06	
	Amps	Inductor Saturation Current	33 Needs to be 60% higher than $I_{\text{CHG(MAX)}}$	
	Inductor Calculations: Power Electronics by Daniel Hart			
	H	$L_{\text{MIN}}$	2.65E-07	
	uH	$L_{\text{MIN}}$	0.264857	
	H	L	4.7E-06	
	uH	L	4.7	Based on proposed ripple current below
	%	$\% \Delta I_L$	22.54	Ripple Current %
	Amps	$\Delta I_L$	3.61E+00	Ripple Current calc'd from spec'd inductor

Table 3) Inductor sizing calculations

Input and output capacitance values are calculated with the help of the datasheet [13], Texas instruments application notes [9] as well as a Power Electronics textbook [14].

Input Capacitor: Texas Instruments publication [9]			
Input Capacitor Calculations	sec	$\tau_{R\_PS}$	0.00004 *based on estimate from sample calculations
	Volts	$\Delta V_{\text{IN\_Trans\_ripple}}$	0.7 *2% of max input voltage
	Amps	$I_{\text{Trans\_step}}$	9.5 *use max current???
	$\Omega$	$ESR_{s <}$	0.18 <input type="checkbox"/> Manufacture stated ESR needs to be less than calc'd value
	$\Omega$	$ESR_{s\_spec\_sheet\_value}$	0.028 *ESR on spec sheet of Bulk Capacitor
	Amps	$\Delta I_{\text{RMS\_max\_ceramic\_capacitors}}$	8.011068 <input type="checkbox"/> capacitor temperature rise should be less than 10°C at
	F	$C_{\text{in} >}$	5.38E-05 <input type="checkbox"/> needs to be compared to DC Bias data of capacitor
	uF	$C_{\text{in} >}$	53.81224 Ceramic Capacitance needed
	Fraction	DC Voltage Bias	0.6
	uF	$C_{\text{in\_DC\_Bias} >}$	86.09959 *Degraded capacitance based on DC Voltage Bias
	F	$C_{\text{Bulk} >}$	6.32E-05 *bulk capacitance suggested Aluminum Electrolytic
	uF	$C_{\text{Bulk} >}$	63.24245 <input type="checkbox"/> needs to be compared to DC Bias data of capacitor
	uF	$C_{\text{Total}}$	149.342
	Volts	$\Delta V_{\text{IN\_PP}}$	0.16 *peak to peak input ripple voltage
	Amps	$\Delta I_{\text{RMS\_max\_bulk\_capacitor}}$	0.257296 <input type="checkbox"/> Aluminum Electrolytic capacitor allowable ripple current needs to be < calculated value
Amps	$\Delta I_{\text{Allowable\_ripple\_current}}$	2.75 *spec sheet data	

Table 4) Input capacitor sizing calculations

Output Capacitor: LTC 4015 Datasheet				
Output Capacitor Calculations	$\Omega$	$ESR_{\text{CBAT}}$	0.01 *based on datasheet	
	Amps	$\Delta I_{\text{PP}}$	3.606565 *references above $\Delta I_L$	
	Volts	$\Delta V_{\text{BAT}}$	0.144 *1% of output voltage	
	F	$C_{\text{BAT}}$	8.35E-06	
	uF	$C_{\text{BAT}}$	8.353609	
	Output Capacitors: Power Electronics by Daniel Hart			
	Volts	$\Delta V_{\text{BAT}}$	0.144 *1% of output voltage	
F	$C_{\text{BAT}}$	6.26E-06		
uF	$C_{\text{BAT}}$	6.261398		

Table 5) Output capacitor sizing calculations

Power dissipation for the MOSFETs is calculated. Tabulated results are shown for the top and bottom MOSFETs used in the buck converter.

N-Channel TOP and BOTTOM MOSFET Calculations			
Infineon BSC010N04LSI (BOTTOM MOSFET)			
	$(1+\delta\Delta T)$	1.1	Assume 1.1 for junction temp of 50°C
$\Omega$	$R_{DS(ON)}$	0.001	Based on datasheet
Coulomb	$Q_{G(TOP)}$	8.7E-08	Based on datasheet
Coulomb	$Q_{G(BOT)}$	8.7E-08	Based on datasheet
F	$C_{RSS}$	1.4E-10	Based on datasheet
Watts	$P_{COND(BOT)}$	0.662967	LTC4015 Datasheet equation
Watts	$P_G$	3.045	LTC4015 Datasheet equation (internal to LTC4015)
Watts	$P_{TRANS}$	0.686	LTC4015 Datasheet equation
Watts	$P_{total}$	1.348967	<b>Total Power Losses</b>
Infineon BSC010N04LSI (TOP MOSFET)			
	$(1+\delta\Delta T)$	1.1	Assume 1.1 for junction temp of 50°C
$\Omega$	$R_{DS(ON)}$	0.001	Based on datasheet
Coulomb	$Q_{G(TOP)}$	8.7E-08	Based on datasheet
Coulomb	$Q_{G(BOT)}$	8.7E-08	Based on datasheet
F	$C_{RSS}$	1.4E-10	Based on datasheet
Watts	$P_{COND(TOP)}$	0.463433	LTC4015 Datasheet equation
Watts	$P_G$	3.045	LTC4015 Datasheet equation (internal to LTC4015)
Watts	$P_{TRANS}$	0.686	LTC4015 Datasheet equation
Watts	$P_{total}$	1.149433	<b>Total Power Losses</b>

Table 6) Mosfet sizing calculations

All of the tabulated result make up the calculations necessary to populate the complete LTC4015 circuit. Key components are highlighted below in the schematic.

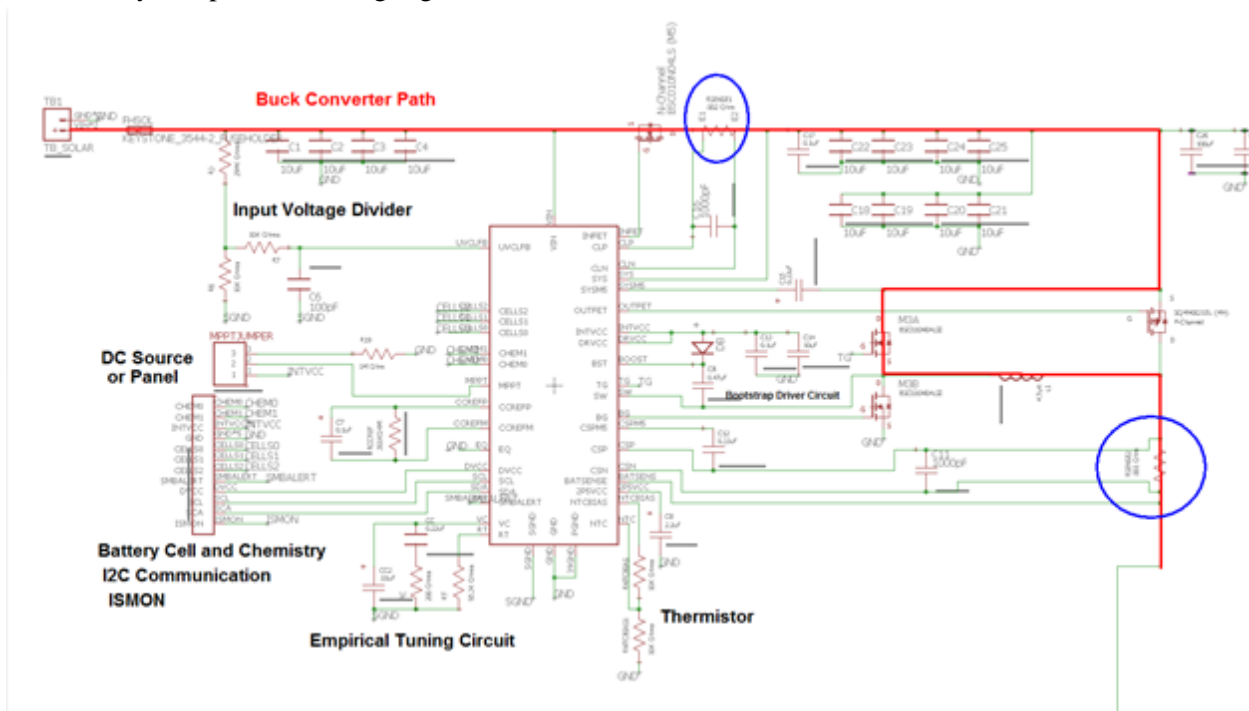


Figure 32) LTC4015 Eagle circuit schematic



## PCB Development

All schematics and components were developed in Eagle software which ultimately allows for the prototyping of the physical board. Seen below is the completed Rev 1 PCB board. Pads for the majority of components were meticulously detailed and constructed in Eagle. All wire traces were run by hand following a similar lay out to Linear's demo boards.

The 4-layer PCB was saved into the necessary Gerber files for manufacturing. Each gerber file represented a different operation conveyed to the manufacture.

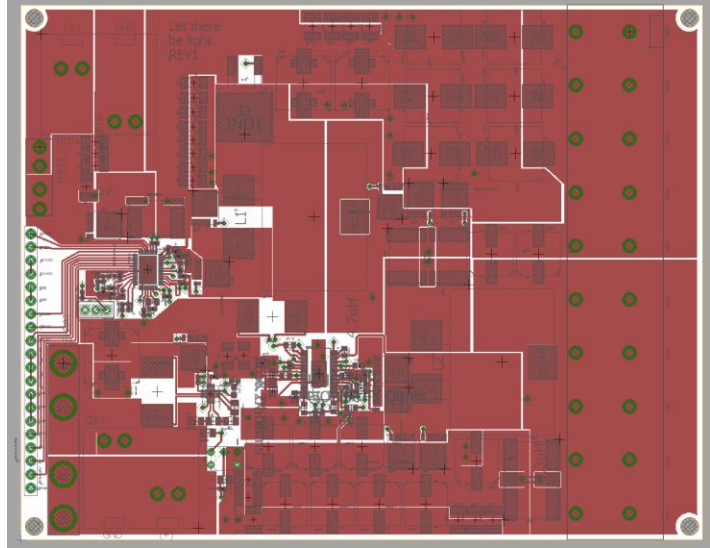


Figure 35) PCB Eagle board Layer 1

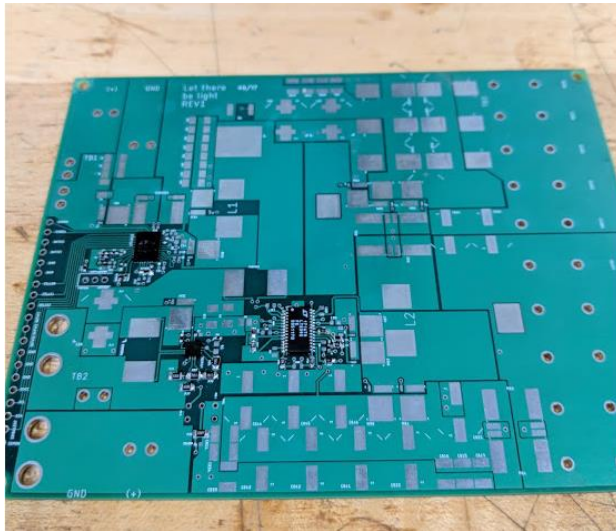


Figure 37) Manufactured PCB with IC's soldered on

For example, there was a drill file for all the through holes specified in the layout. A silkscreen layer for all the labeling of pads and component locations. Traces had separate files for each layer. The totality of these files represented the necessary details for the manufacture to produce the board seen in Fig. 5. Bay area circuits was the manufacture chosen based on proximity, speed and price.

The next task was to order all the components and organize them. The IC's were the first components attached to the board. First the pads for the IC components were tinned meaning flux was wiped on the pads then solder applied to the tip of a soldering iron. Finally the tip was run across the pads and the flux helped to congregate the solder only on the metallic pads. A hot air soldering tool was placed below the PCB to heat it from the bottom while a second was held and pointed from the top to apply even heating to the IC and PCB board so a consistent temperature was shared between the two. After some patience the solder melted and became liquid pulling metallic surfaces towards eachother. Pads on the underside of the IC were attracted to the mirrored pads on the PCB. Surface tension would then pull the IC so the pads were on top of one another with a thin liquid solder layer in-

For example, there was a drill file for all the through holes specified in the layout. A silkscreen layer for all the labeling of pads and component locations. Traces had separate files for each layer. The totality of these files represented the necessary details for the manufacture to produce the board seen in Fig. 5. Bay area circuits was the manufacture chosen based on proximity, speed and price.

The next task was to order all the components and organize them. The IC's were the first components attached to the board. First the pads for the IC components were tinned meaning flux was wiped on the

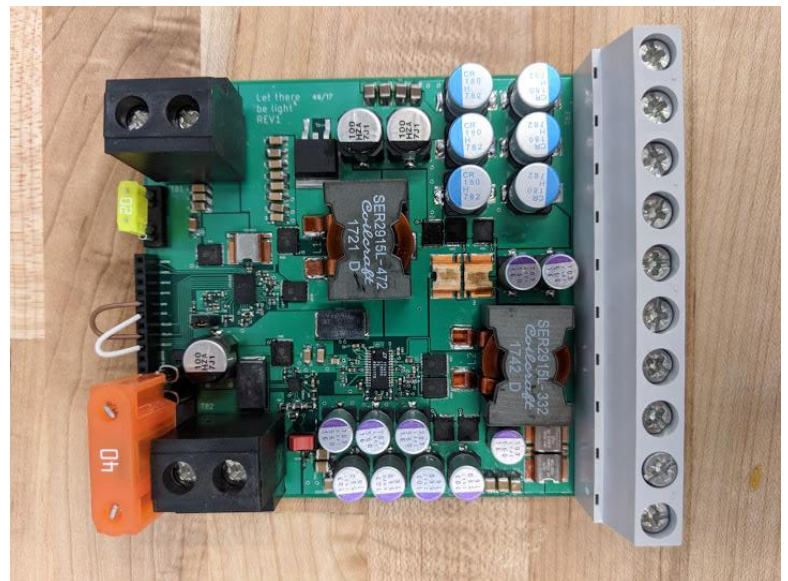


Figure 36) Populated PCB board

between. The surface tension and amount of solder used also prevented bridging between pads. The IC could be pushed slightly with tweezers while the solder was liquid and it would snap back into place. This ensured that the pads were contacting the correct spot on the IC. Once the IC was in the correct orientation and position the hot air tool was slowly removed, ensuring a slow cooling rate. The process was repeated for all 3 IC's.

Soldering of the smallest 0402 surface mount components came first. The order of operations followed a similar pattern of smallest to largest components. A collection of youtube videos can be found for soldering various component sizes and types.

Unfortunately, after all fabrication and soldering of the PCB board was complete testing turned catastrophic. While using a constant DC source the charge controller failed to limit or regulate the voltage at 12 Volts as expected. Instead the output voltage continued to climb. Around 20 Volts a component failed with a pop and the system shorted at the input. Significant time was spent troubleshooting however based on the aggressive timeline set forth the decision was made to use a readily available charge controller on the market.

## 2.2 Fabrication

### Electrical System

The electrical system developed for the mobile residence needed functionality required by modern habits. The tabulated components used are listed in Tab.7. Development and fabrication of each component is discussed in detail.

### Electrical Containment Box

Much of the electrical assembly was housed in an electrical containment box. Steel square tubing (1 in x 1inch x 0.0625 in) was the structural framing used. The component platform was a flame retardant and nonconductive PVC base. Initially the large components were modeled in Creo 2.0. The CAD model made it easy to iterate location of components preventing unused space. Below is the assembly CAD model which finalized dimensions of the electrical containment box.

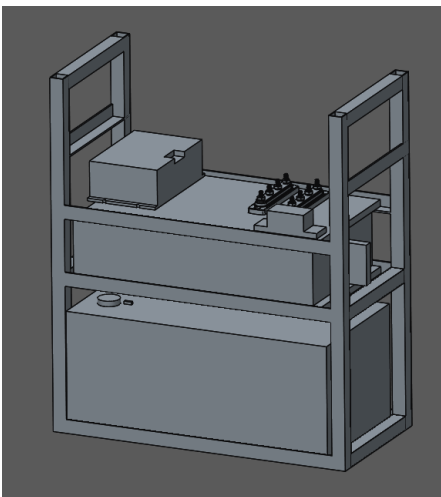


Figure 40) Electrical containment box populated with large components

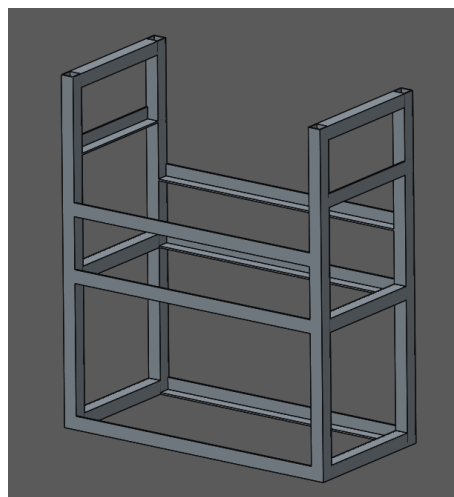


Figure 39) Electrical containment box framing



Figure 38) Fabricated and populated electrical containment box

A final drawing of the weldment was necessary to convey dimensions, tube geometry, and bulk material needed for the fabrication.

Once fabricated electrical components could easily be mounted to the 1/4-inch-thick PVC by cutting threads with a tap and directly mounting components via fasteners. The top shelf served this purpose and Fig. 7 illustrates the components that were mounted.

### Solar Panel Frame Fabrication

After the solar panels were specified based on energy consumption specified they needed to be installed on the roof of the mobile residence. Roof rails were installed and sealed on the roof so frames could be attached to the vehicle. Measurements were taken of the roof rails and a solid model was created in Creo 2.0 to describe the allowable mounting zone for the panels and surface area available for the panels. A frame was constructed of readily available steel tubing and angle iron dimensions. Protective shrouds were made of plate steel to protect the panels at the corners from any uncalculated collisions on the road or while parked. The panels were repeatedly checked to ensure they would fit the frames in the CAD model. Figure 12 illustrates the assembly which included the solar panels, critical mounting locations, both frames and roof rails.

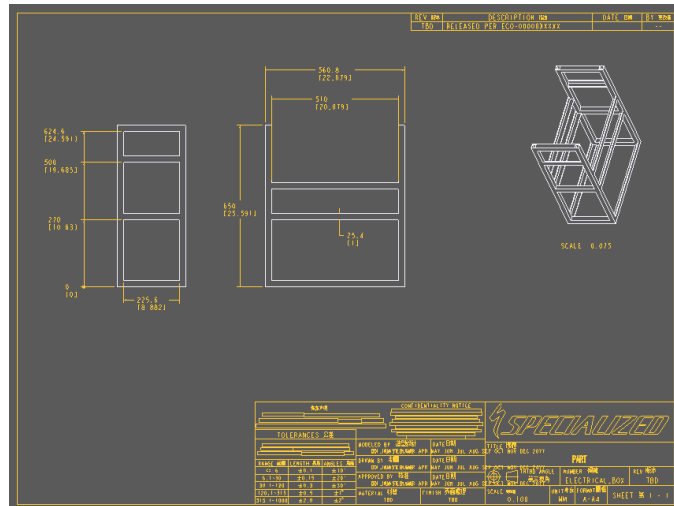


Figure 41) Electrical containment box drawing for fabrication

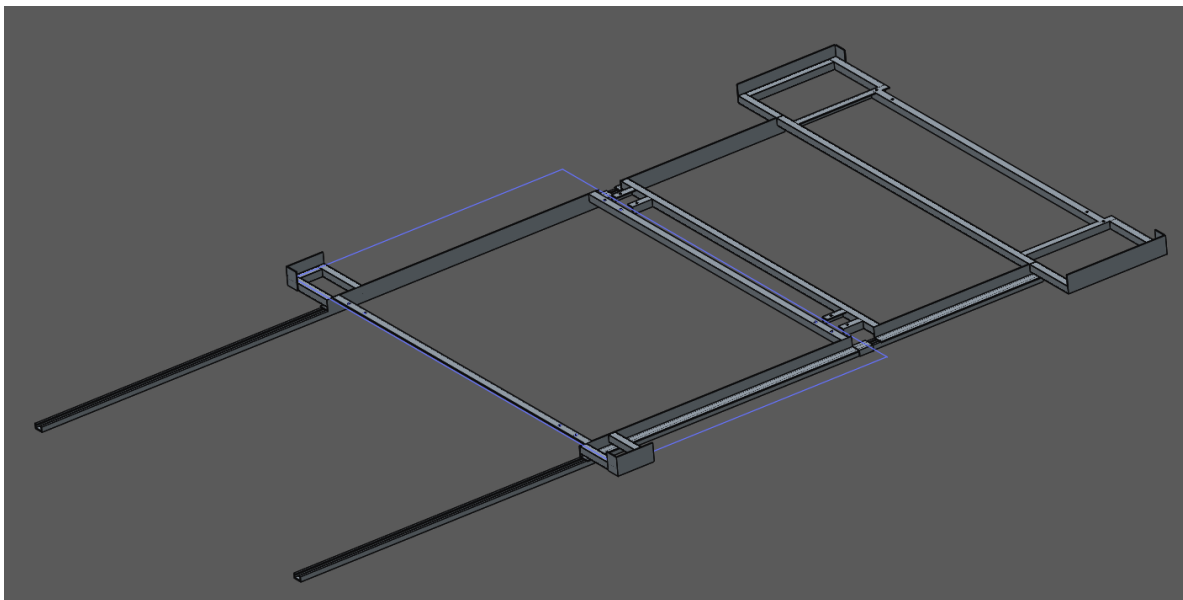
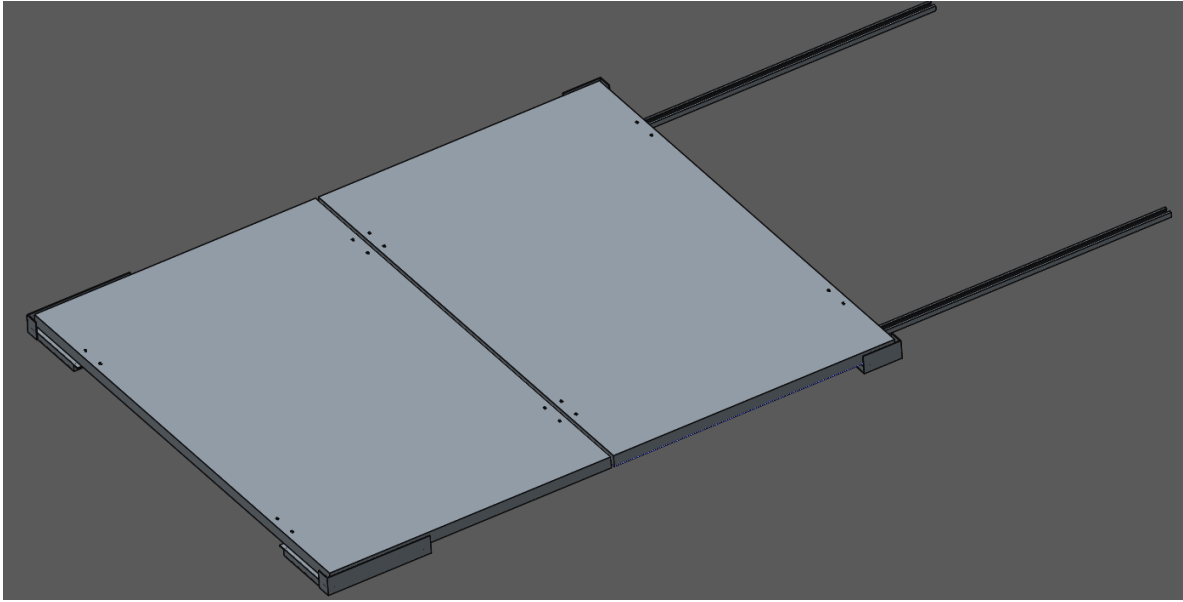
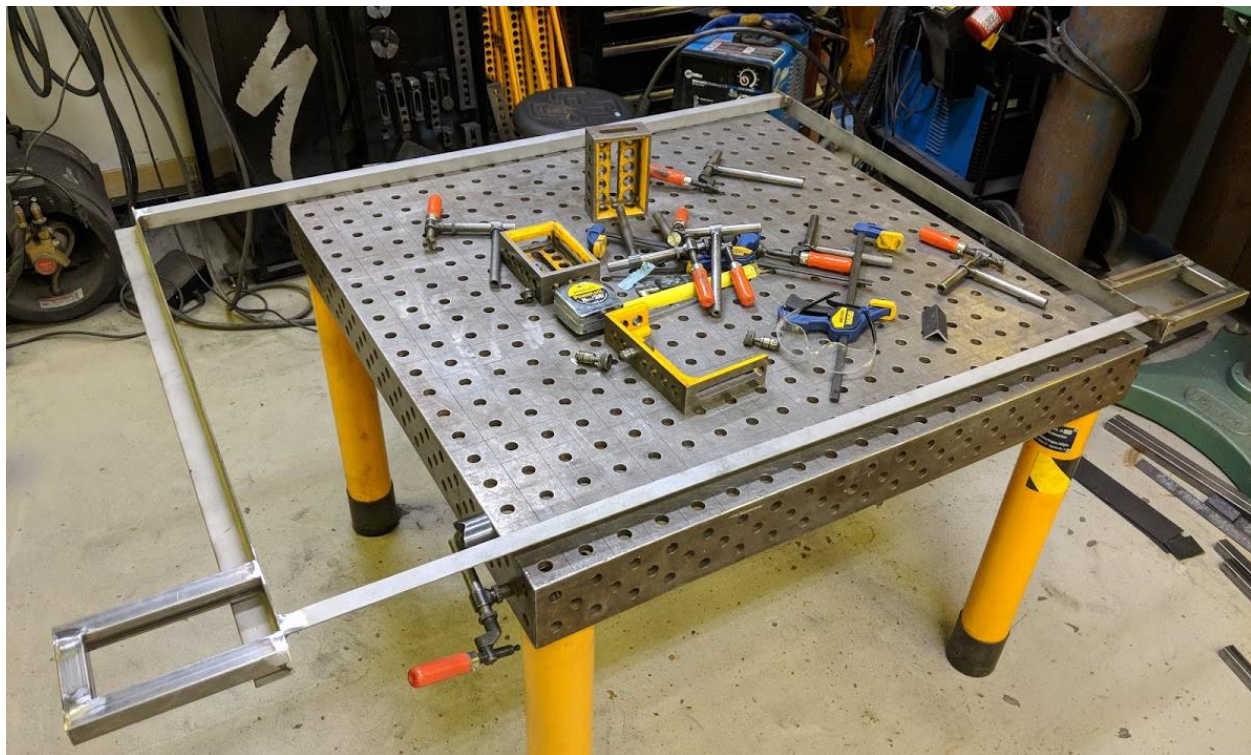


Figure 42) Solar panel frame CAD model



*Figure 43) Solar frame CAD assembly*

A final frame drawing was fabricated based on these CAD models. Tube geometry was included along with dimensions to ensure the correct amount of material was ordered for fabrication. Mild steel in 2 x 0.125 inch angle iron and 1 x 1 x 0.0625 inch square tubing was used. Mild steel was attractive because it was readily available in sizes needed, inexpensive, durable, and easy to weld for a novice. Aluminum would have been an ideal choice but because of the expertise needed to weld thin wall tubing it was avoided. However, the potential weight savings from aluminum made it an attractive option.



*Figure 44) Front frame mid welding operation*

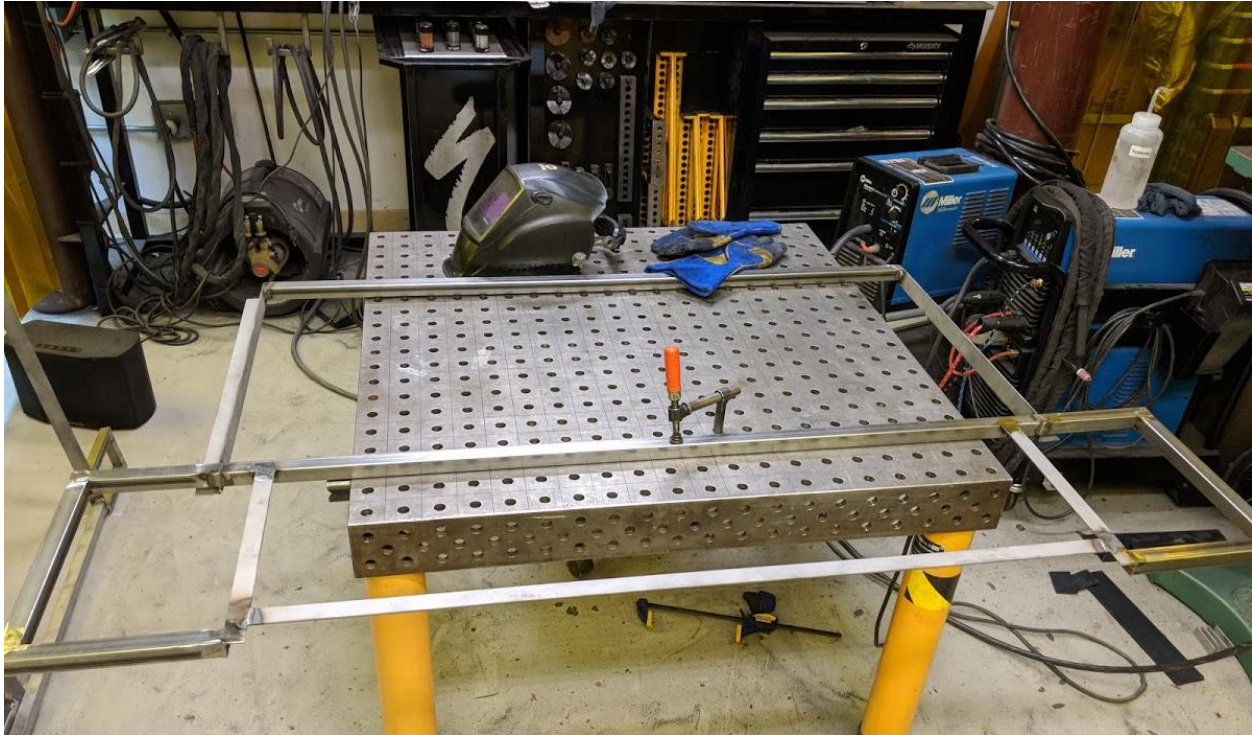


Figure 45) Rear frame mid welding operation

Solar Frame Assembly

The solar panel frame was mounted to the T-slot of the roof rails via short headed fasteners. The solar panels were then fastened to the roof following the recommendation provided by Canadian solar in their mounting handbook [20]. Wiring was run by drilling holes in the roof adequately sized to run 6 AWG wire. A grommet was used along with M3 roof sealant to seal the breach from any water or contaminants getting in via the holes. A protective cover was then used to further cover the holes and fix the wires in position. The protective cover was mounted via M5 fasteners and sealed using M3 roof sealant, all while being positioned under the solar panels to prevent UV corrosion of the plastic. The panels were connected in parallel on the roof seen in Fig. 15 to limit the amount of wires entering.



Figure 46) Solar wiring



Figure 47) Solar Mounting

### Victron Charge Controller

After facing issues designing a charge controller a suitable option was found on the market from Victron. The SmartSolar MPPT 100/30 had a maximum input of 100 volts and output of 30 Amps. In the future the 100/50 option would be purchased because at a nominal 13.4 Volts output for the battery and 30 Amp max the power is limited to 402 Watts, on average. Even though the panels can pull in a maximum of 550 Watts the charge controller will limit this within its bounds. The 100/50 option from Victron would have been a better fit to the system.

The available mobile app and data present to the user made the Victron charge controller attractive. Current state data such as solar wattage being pulled in and battery voltage and current could all be viewed on a mobile phone. The app also allowed access to information for the past 30 days such as daily solar yield and maximum battery voltage.

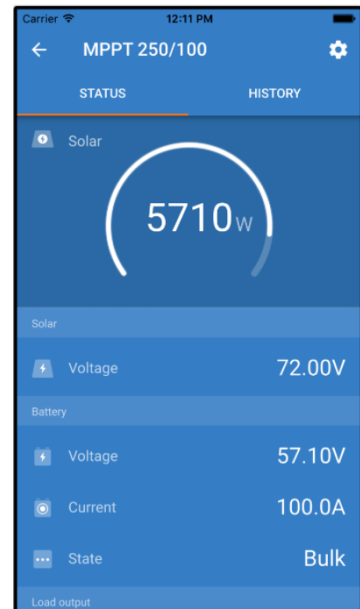


Figure 48) App home screen for Victron MPPT 100/30

### Various Electrical Components

The BMV-712 by Victron was used to monitor the SOC of the battery and historical charge voltages. A battery protect relay was also used in conjunction with the BMV-712. When the SOC drops below 10% the relay is activated and the battery protect disconnects the 12 Volt line ensuring the battery is not discharged past an unsafe level. The 12 Volt load line is also fused for various levels of loads to be connected in the future. The inverter has a continuous draw capacity of 2000W and a peak of 4000W. The inverter as well as the battery have switches which allow a user to manually disconnect each from the system. Table 7 lists the relative components and Fig. 17 illustrates the construction.

Electrical Model		
Designator	Components	Description
1	LiFePO4 Battery	260 Amphr battery
2	Solar Panels	Quantity (2) 275-Watt panels wired in parallel
3	Charge Controller	Victron MPPT SmartSolar 100/30
4	Battery Management	Victron BMV-712 monitors battery SOC and historical voltages
5	Battery Protect Relay	Relay connected to BMV, once SOC < 10% system loads are disconnected
6	Inverter	12V DC to 120 V AC 2000W continuous, 4000W pulse
7	Safety Switches	Cut off for battery and inverter
8	12V Fused Load Line	For miscellaneous 12V DC loads
9	120V AC line	For miscellaneous 120V AC loads
10	Air Conditioner	Not installed

Table 7) Electrical components housed

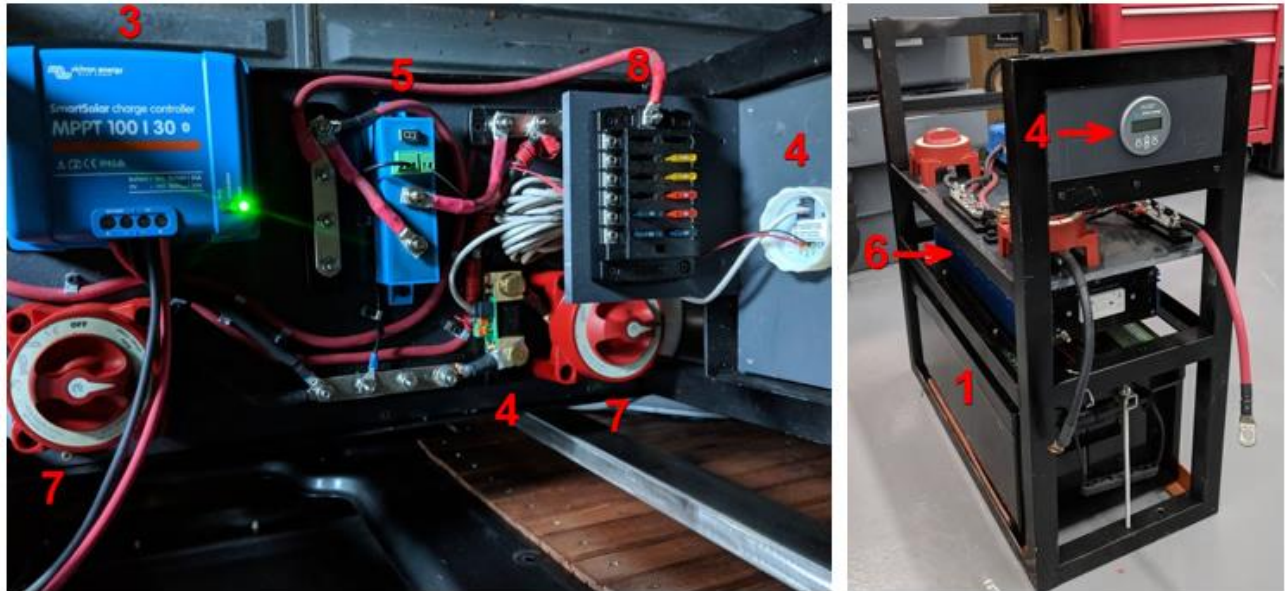


Figure 49) Electrical components in electrical containment box

## 2.3 Thermal Model

### First Order System

To predict the internal temperature of the mobile residence in different thermal conditions a theoretical model is needed. A simplified first order approach is a logical initial starting point. Equation 2.3.1 is used in the energy management of buildings [19] and applied in our case to a mobile residence. To solve for internal temperature: external temperature,  $U_{sun}$ , and the respective alpha coefficients are needed. It should be noted that initially  $U_{ac}$  was set to zero because the internal temperature was not influenced by an air conditioner.

A data acquisition tool comprised of two LM35 temperature sensors, a photoresistor, and Arduino Uno was constructed. The DAQ interfaces with publicly available software from PLX that records values from the Arduino microcontroller into excel. The two temperature sensors are used to collect internal and external temperature data, while the photoresistor quantified the intensity of sunlight on the mobile residence. Ultimately the internal temperature recorded will be used to verify the accuracy of the model which is the next discussion below.

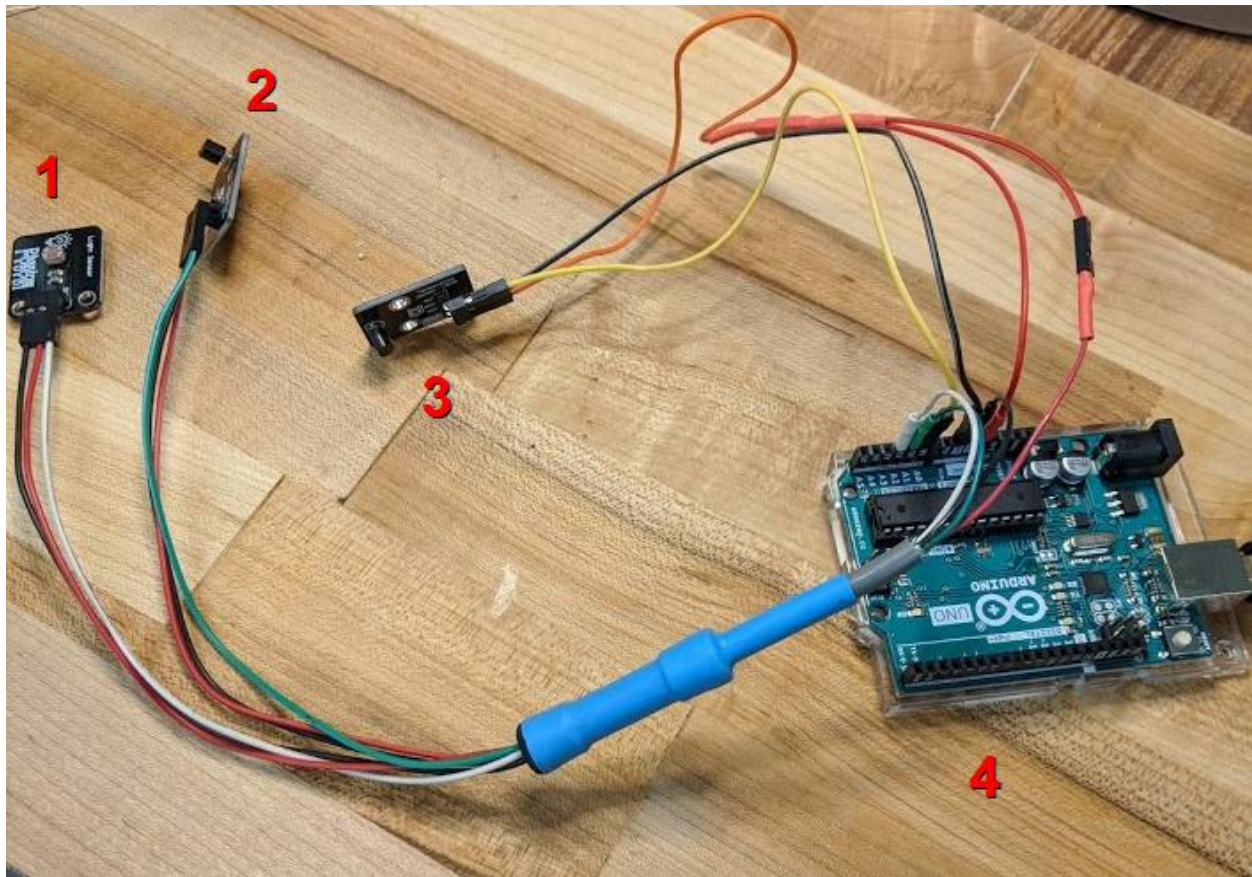


Figure 50) Thermal data acquisition tool

$$\frac{dT}{dt} = \alpha_{a1}(T_{\infty} - T) + \alpha_{sun1}U_{sun} + \alpha_{ac}U_{ac} \quad (2.3.1)$$

Internal temperature, external temperature, and sunlight data were collected over an 11-hour period. Using the first order differential Eq. 2.3.1 a predicted or theoretical internal temperature could be computed throughout the 11-hour period and compared to the actual collected data. First the differential equation was discretized using the forward difference method.

$$T^{k+1} = T^k + \Delta t^k [\alpha_{a1}(T_{\infty}^k - T^k) + \alpha_{sun1}U_{sun}^k + \alpha_{ac}U_{ac}^k] \quad (2.3.2)$$

We will call the collected internal temperature data  $T_{real}$  and the predicted theoretical temperature from the first order model  $T_{model}$ . For predictions we needed to assign values for the alpha coefficients. MATLAB is employed using the `fminsearch` function to iterate through possible values and minimize the error produced by each value.

Using the least squares method, we can compute the relative error at every data point collected throughout the day ( $T_{model} - T_{real}$ ). Then square and sum these values to quantify the total error in our predicted model. We will call this quantified error  $J$ . The goal is to minimize the error by varying the alpha parameters in the first order equation. Using the `fminsearch` function in MATLAB hundreds of iterations are run until the convergence criteria is met. The final minimum value of  $J$  for the first order equation is 4281.2

$$J = \sum_{k=1}^N (T_{model} - T_{real})^2 \quad (2.3.3)$$

$$J_{min} = 4281.2$$

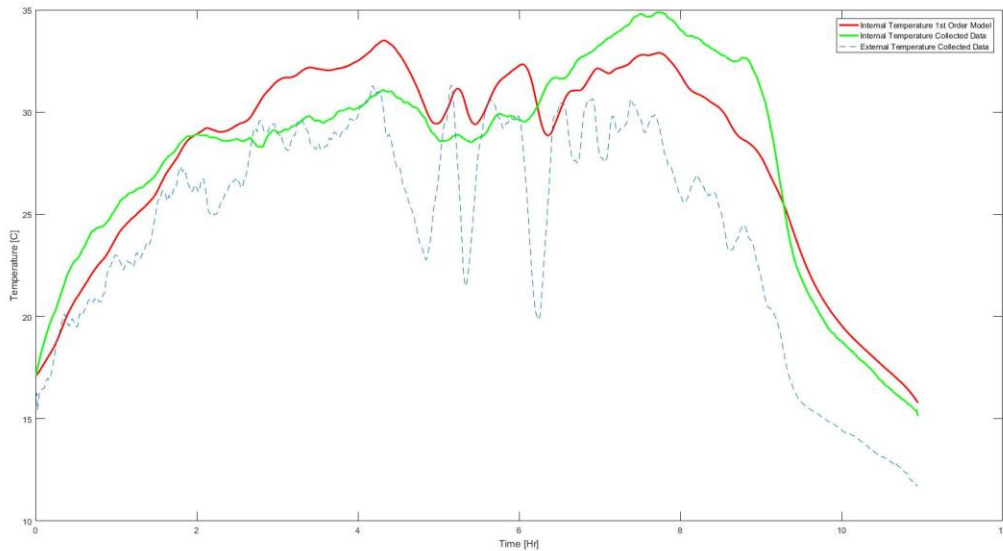


Figure 51) First order internal temperature approximation and actual internal temperature data

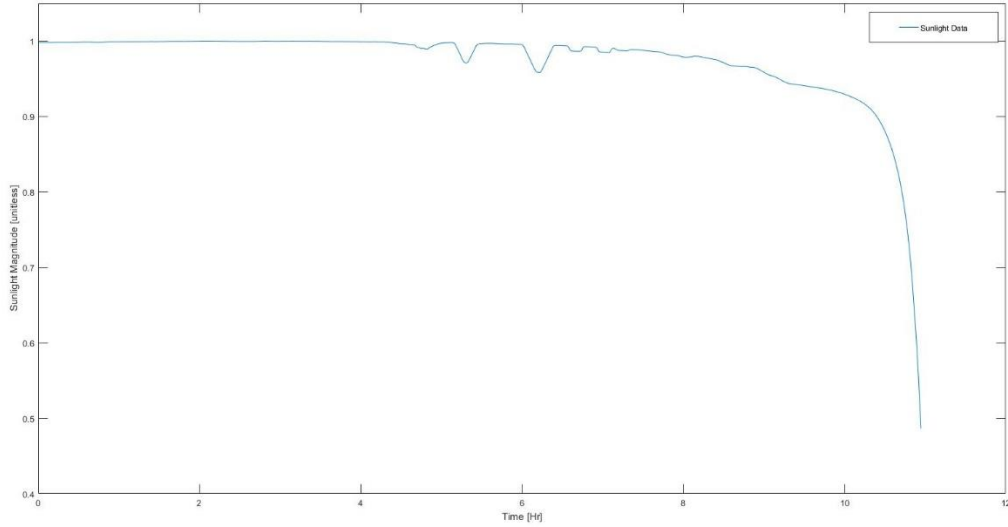


Figure 52) Saturated sunlight data

$T_{\text{model}}$  and  $T_{\text{real}}$  are plotted to illustrate the difference that  $J_{\text{min}}$  describes. It can be seen from Fig. 19 that the model and real values deviate from one another throughout the 11 hour period. A more accurate  $T_{\text{model}}$  approximation was obtained by using a second order approach.

### Second Order System

To increase the accuracy of the predicted internal temperature a second order approach was used by introducing the wall temperature.  $T_w$  is the average temperature of the wall assuming no temperature gradient across the thickness. The walls have some thermal capacitance and the 2<sup>nd</sup> order approach helps to capture these dynamics.

$$\frac{dT}{dt} = \alpha_{w1}(T_w - T) + \alpha_{a1}(T_{\infty} - T) + \alpha_{sun1}U_{sun} + \alpha_{ac}U_{ac} \quad (2.3.4)$$

$$\frac{dT_w}{dt} = \alpha_{w2}(T - T_w) + \alpha_{aw}(T_{\infty} - T_w) + \alpha_{sun2}U_{sun} \quad (2.3.5)$$

The 2<sup>nd</sup> order equations are discretized by the forward difference approximation. The discretized equations used in the MATLAB code are below.

$$T^{k+1} = T^k + \Delta t^k [\alpha_{w1}(T_w^k - T^k) + \alpha_{a1}(T_{\infty}^k - T^k) + \alpha_{sun1}U_{sun}^k + \alpha_{ac}U_{ac}^k] \quad (2.3.6)$$

$$T_w^{k+1} = T_w^k + \Delta t^k [\alpha_{w2}(T^k - T_w^k) + \alpha_{aw}(T_{\infty}^k - T_w^k) + \alpha_{sun2}U_{sun}^k] \quad (2.3.7)$$

Again, the function  $J$  is minimized by varying the alpha coefficients and taking advantage of the `fminsearch` function available in MATLAB. Showing improvement compared to the first order approach the function  $J$  has a minimum value of 3547.3

$$J_{\text{min}} = 3493.9$$

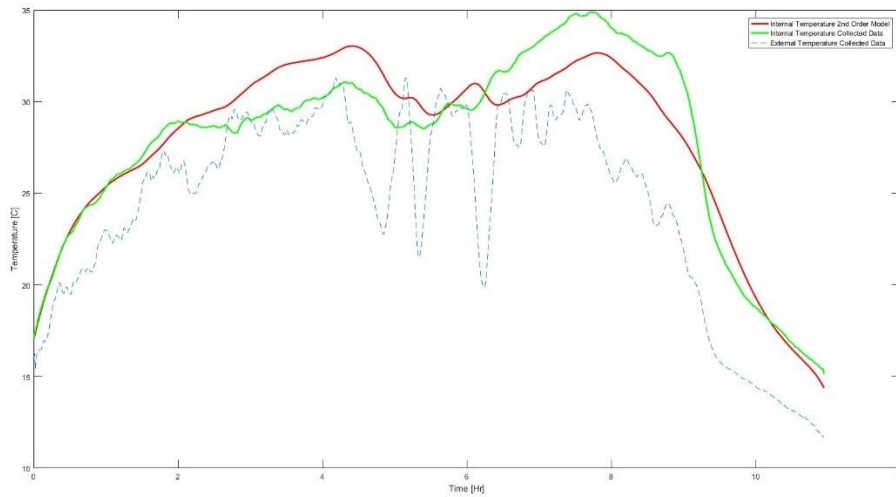


Figure 53) Second order internal temperature approximation and actual internal temperature data

### Second Order System with UV index data

It is shown that the sunlight data for the 11-hour period is saturated throughout most of the day in Fig. 22. Another approach to further optimize the internal temperature model was to use UV index data gathered from wunderground.com. The data was pulled from the website and plotted. The  $U_{sun}$  term in the 2<sup>nd</sup> order discretized equation was then set equal to the UV index data. The alpha terms were then found using the same methodology described above. As illustrated below the model has the best approximation and  $J_{min}$  is the lowest seen by any other method.

$$J_{min} = 2003.2$$

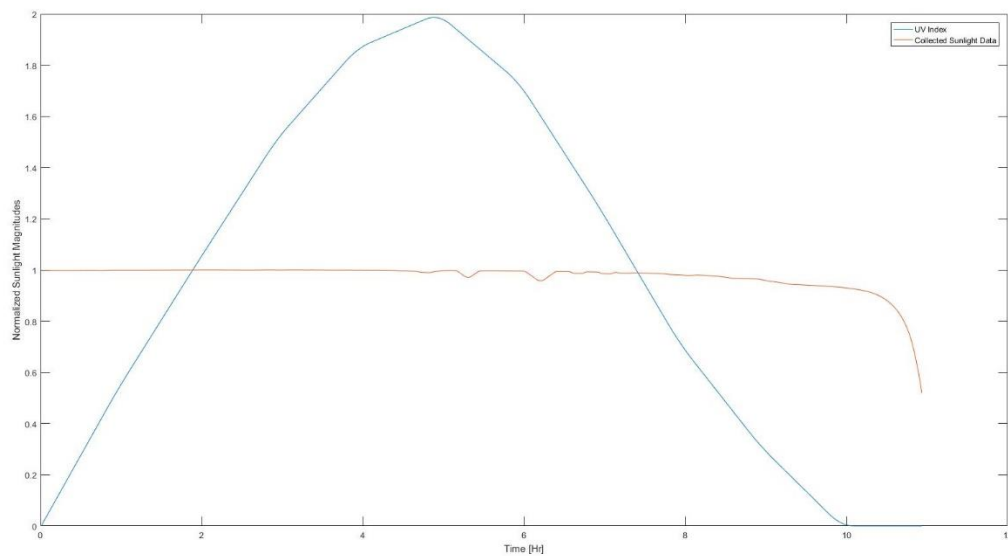


Figure 54) Saturated sunlight data and UV index data

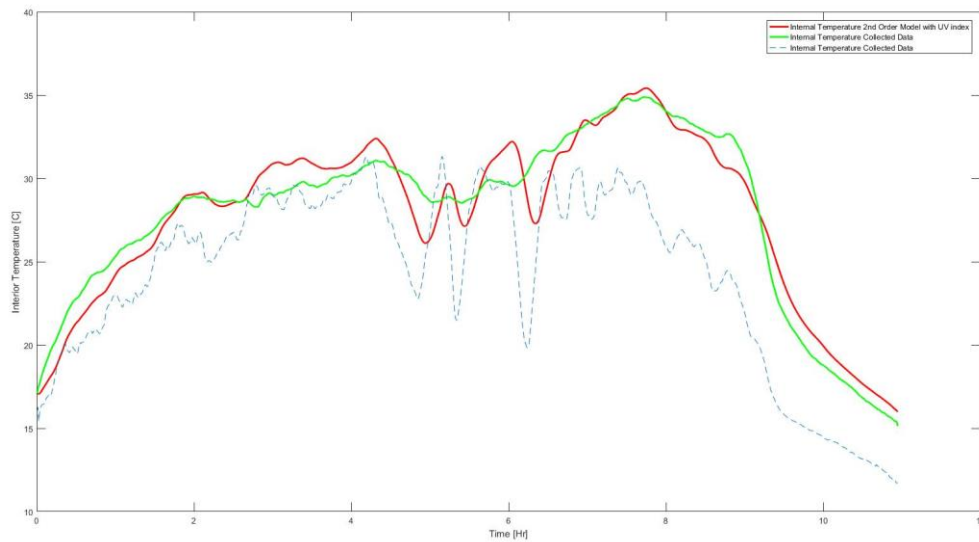


Figure 55) Second order internal temperature approximation from UV data and actual internal temperature data

## 2.4 API to Wunderground

It was quickly skimmed over that UV index forecast data was used. To obtain this information an API was written in MATLAB to communicate with wunderground.com [22]. The following code in Fig. 24 accessed external temperature and UV index data for a user specified location. The data has an hourly time step. The MATLAB code grabs data for the following 60 hours. However, since the timestep of the thermal model is every minute the data from wunderground needed to be interpolated to fit the thermal model timestep. The data is interpolated using the MATLAB function `interp1()`.

```

%%API Wunderground
key = '22d6314cfd649ff8';
options = weboptions('ContentType','json');

CallURL_forecast = ['http://api.wunderground.com/api/22d6314cfd649ff8/hourly10day/q/CA/Morgan_Hill.json'];
Forecast_Data = webread(CallURL_forecast, options);
disp('Forecast');

tempstruct = cat(1,Forecast_Data.hourly_forecast.temp);
CompleteTforecast = str2double({tempstruct.metric}');
Tforecast = CompleteTforecast(1:60)+10;
time = (0:1:(length(Tforecast)-1))';

Condition = {Forecast_Data.hourly_forecast.condition}';
UV1 = str2double({Forecast_Data.hourly_forecast.uvi}');
UV = UV1(1:60);

```

Figure 56) API code

## 2.5 UV index to Solar Irradiance

For the electrical model current obtained from the solar panels is also needed. It is shown that the UV index data is closely correlated to the Solar Irradiance at a specified location. Because solar irradiance

forecasted data is not available via wunderground a relationship between the UV index and proposed solar irradiance was found. The fminsearch function was utilized in MATLAB to find the alpha coefficients for a 2<sup>nd</sup> order approximation of the solar irradiance given the UV index data. The equation solved for is below. The UV index for a given day is plotted as well as the corresponding predicted Solar Irradiance and Actual Solar Irradiance data.

$$\text{Solar Irradiance Predicted} = \alpha_1(\text{UV index}^2) + \alpha_2(\text{UV index}) + \alpha_3 \quad (2.3.8)$$

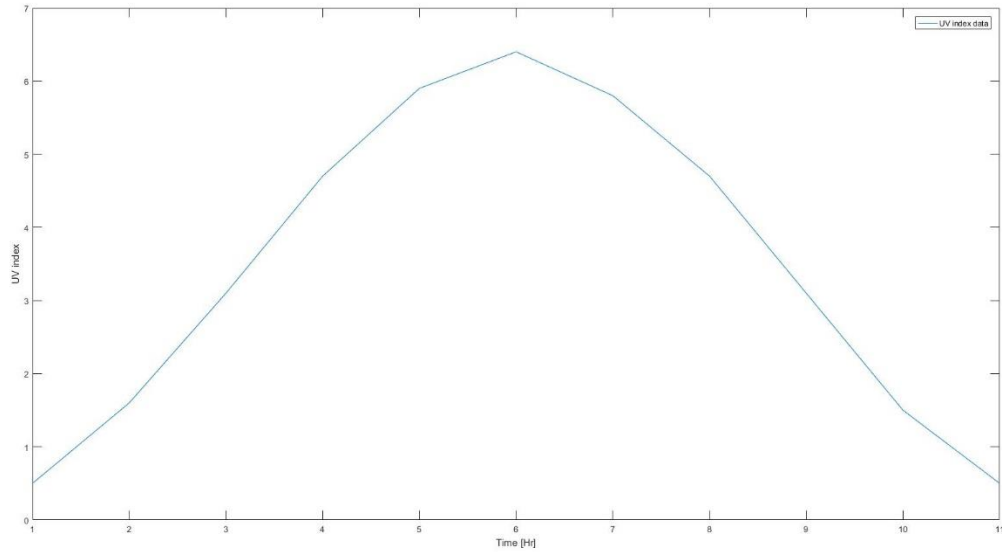


Figure 57) UV index data

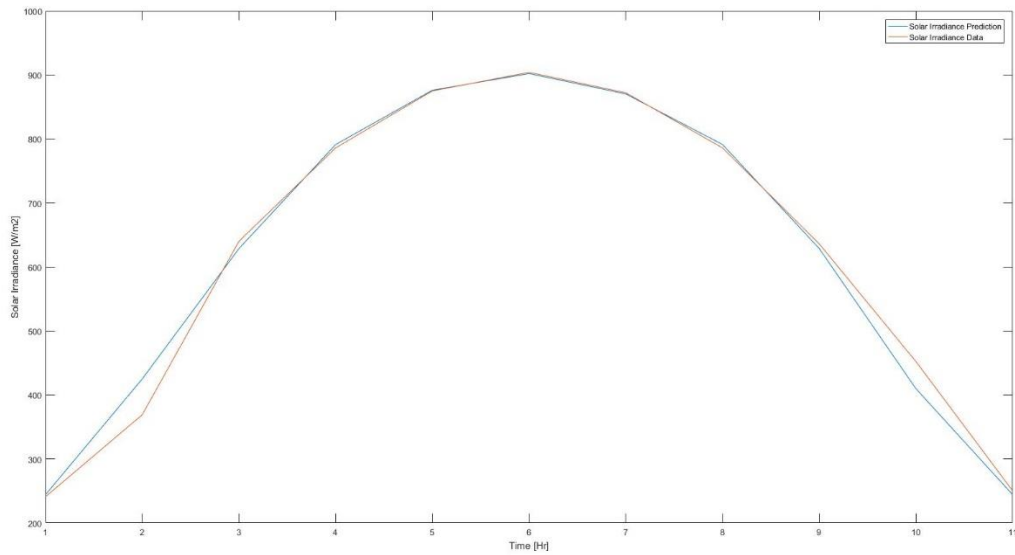


Figure 58) UV index data to Solar Irradiance

The solar irradiance could then be used to calculate the estimated current being pulled into the charge controller and ultimately delivered to the battery or loads. Since the charge controller employs a MPPT

CS6K-270M / I-V CURVES

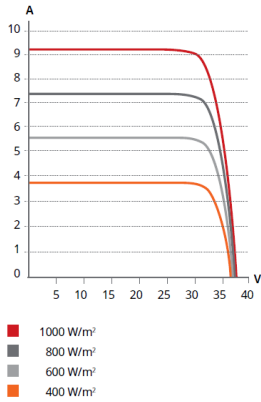


Figure 60) Manufacture publish I-V curves

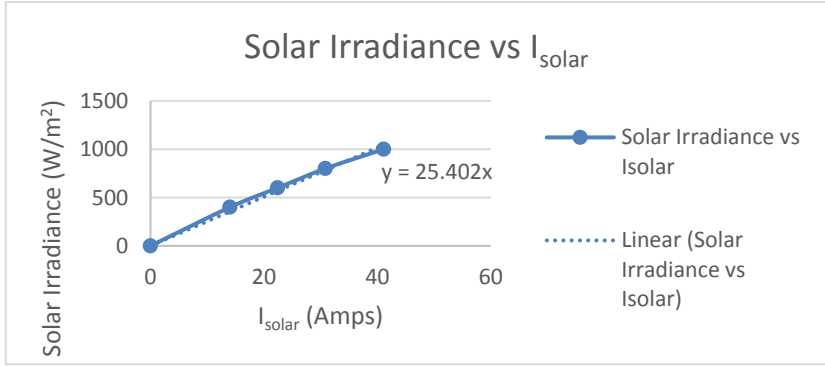


Figure 59) Solar Irradiance to Isolar relationship

charging algorithm it is assumed that the solar panels can be modeled as a current source that is a function of solar irradiance. Using the I-V curves provided by Canadian Solar assuming the panels are held at MPPT of 31.3 Volts current as a function of solar irradiation can be found. The current is then converted to a nominal 13.4 Volts by the charge controller at an assumed 90% efficiency. The current  $I_{solar}$  as a function of Solar Irradiance is known as a linear relationship plotted with the best fit line shown. There for an ideal approximation is made by dividing the solar irradiance by 25.4 will yield the expected  $I_{solar}$  current.

Quantity 2 Panels in Parallel		
Solar Irradiance (W/m <sup>2</sup> )	$I_{panels}$ (Amps) @31.3 Volts	$I_{solar}$ (Amps) @13.4 Volts (90% efficiency)
1000	17.6	41.11
800	13.2	30.83
600	9.6	22.42
400	6	14.01
0	0	0

Table 8) Tabulated solar irradiance to current relationships

### Electrical Model

Ultimately the thermal model developed for the van was used in conjunction with an electrical model. The tabulated components of the electrical build out were described earlier however the theoretical model for simulation was simplified to the following schematic.

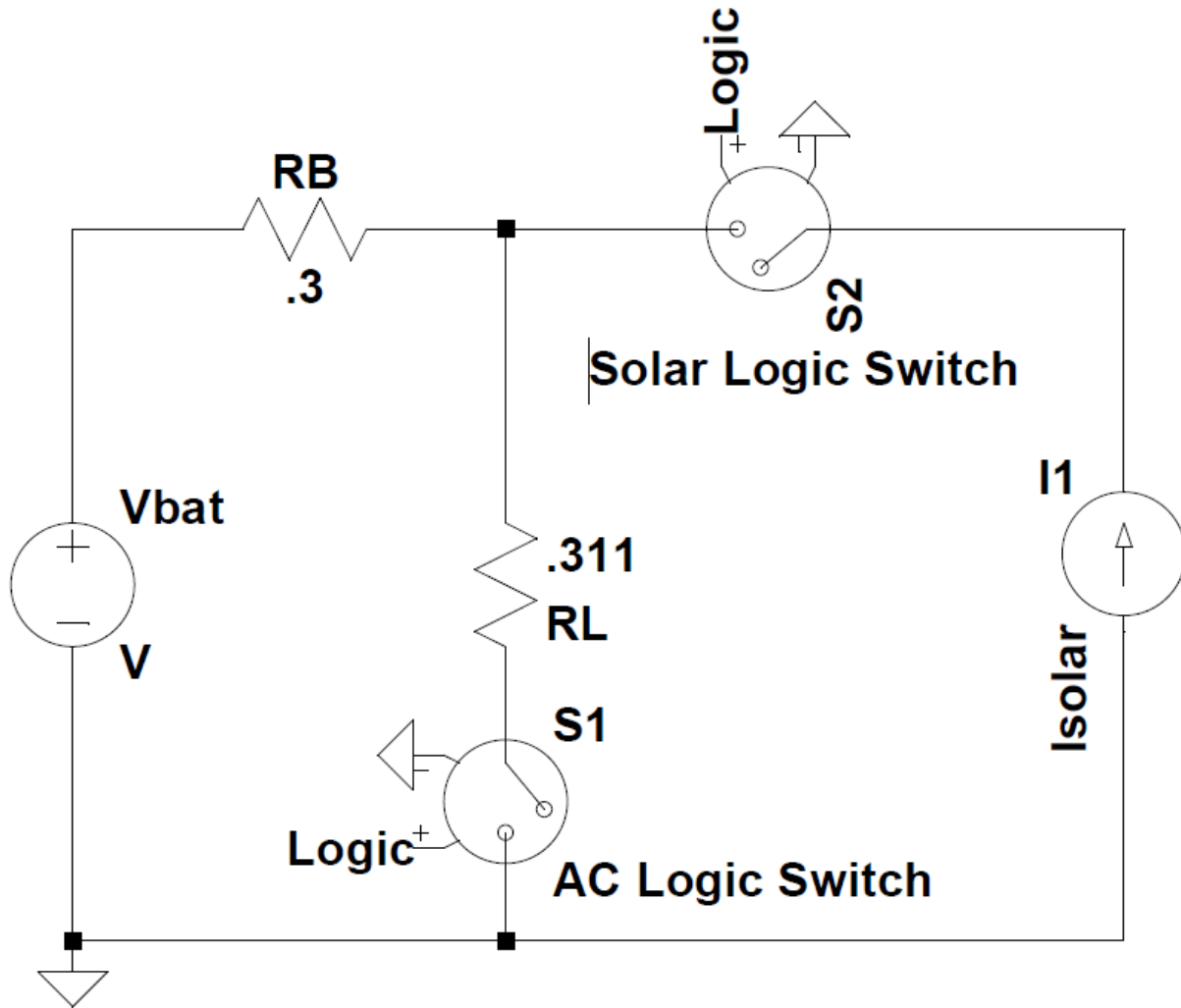


Figure 61) Simplified electrical model

Switch 1 and switch 2 followed the logic flow seen in Fig.31. If the internal temperature is greater than the user set point temperature plus some user specified dead band switch 1 would turn on which simulates the air conditioner load being on. If the internal temperature drops below the set temperature minus some dead band switch 1 would be turned off. If the temperature is within the set point temperature plus or minus the dead band, the switch would remain at its previous position. Switch 2 controlled the input current from the solar panels and was a function of the UV index because  $I_{solar}$  was a function of the UV index. If  $I_{solar}$  was greater than zero switch 2 was turned on, otherwise switch 2 was disconnected. Also, if the SOC of the battery was greater or equal to its max value the solar panels were disconnected by opening switch 2 to prevent over charging of the battery. Likewise switch 1 is left open if the battery is below the user specified threshold.

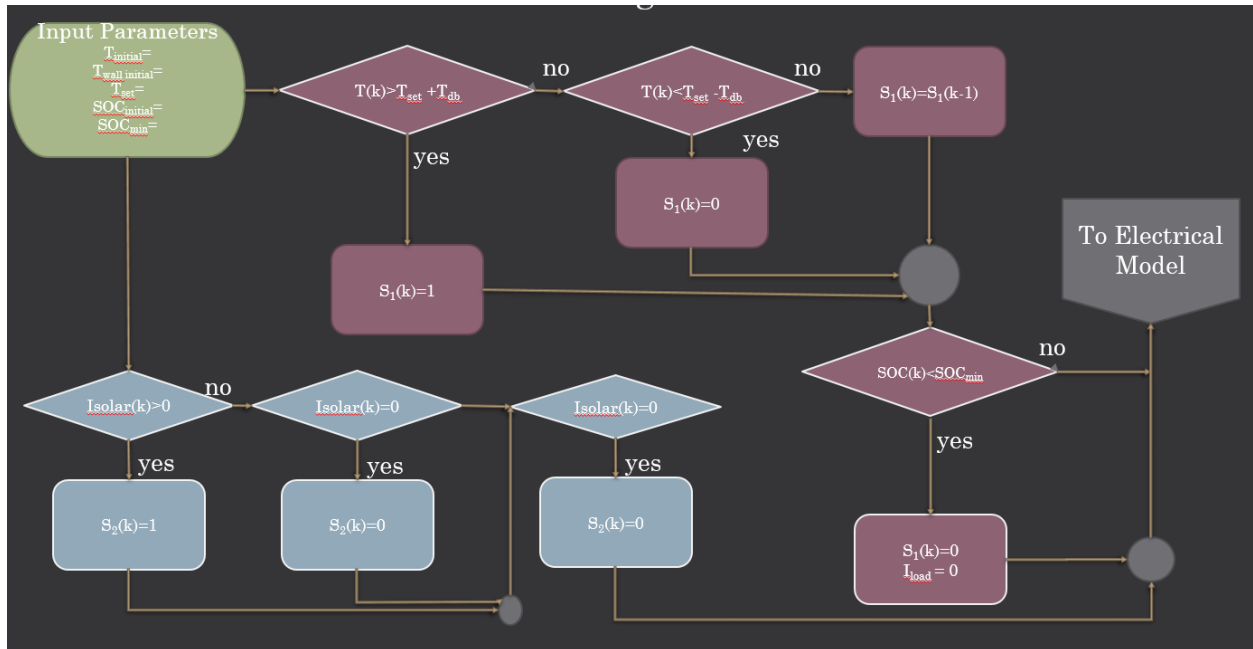


Figure 62) Switch states logic

Once the state of switch 1 and 2 are known the circuit schematic can be solved for four each switch scenarios. Using KVL we can write the equation below and solve for our unknown  $i_b$ . The battery current will be used to determine the battery state of charge. Following the procedure for each scenario the following equations are found.

$$S_1(k) = 1, S_2(k) = 1$$

$$V_{oc}(k) = i_b(k) \cdot R_{bat} + R_{Load} \cdot (i_b(k) + i_{solar}(k)) \quad (2.3.9)$$

$$S_1(k) = 1, S_2(k) = 0$$

$$V_{oc}(k) = i_b(k) \cdot (R_{bat} + R_{Load}) \quad (2.3.10)$$

$$S_1(k) = 0, S_2(k) = 1$$

$$i_b(k) = -i_{solar}(k) \quad (2.3.11)$$

$$S_1(k) = 0, S_2(k) = 0$$

$$i_b(k) = 0 \quad (2.3.12)$$

An idealized  $V_{oc}(SOC)$  is used. We assume the  $V_{oc}$  of the battery is linear function of SOC. Based on the parameters of the battery voltages from the manufactures an ideal linear relationship is found to be.

$$V_{oc}(k) = \frac{15}{9} \cdot SOC(k) + 12.833 \quad (2.3.13)$$

Based on the conditions of battery current and SOC at the current timestep the state of charge at the end of the timestep is calculated as follows. It should be noted that  $i_b(k)$  is assumed positive when discharging the battery.

$$SOC(k + 1) = SOC(k) - \frac{\Delta t \cdot i_b(k)}{Q} + i_{load} \quad (2.3.14)$$

$$Q = (260 \text{ Amp} \cdot \text{hrs}) \cdot \frac{3600 \text{ sec}}{1 \text{ hr}} \quad (2.3.15)$$

### 3.0 Results and Discussion

#### 3.1 Predictive Model with Intelligence

The electrical and thermal models are both incorporated into a single MATLAB script to predict the internal temperature of the mobile residence over a 60-hour period. The logic of the MATLAB code is illustrated below in the flow chart in Fig.31.

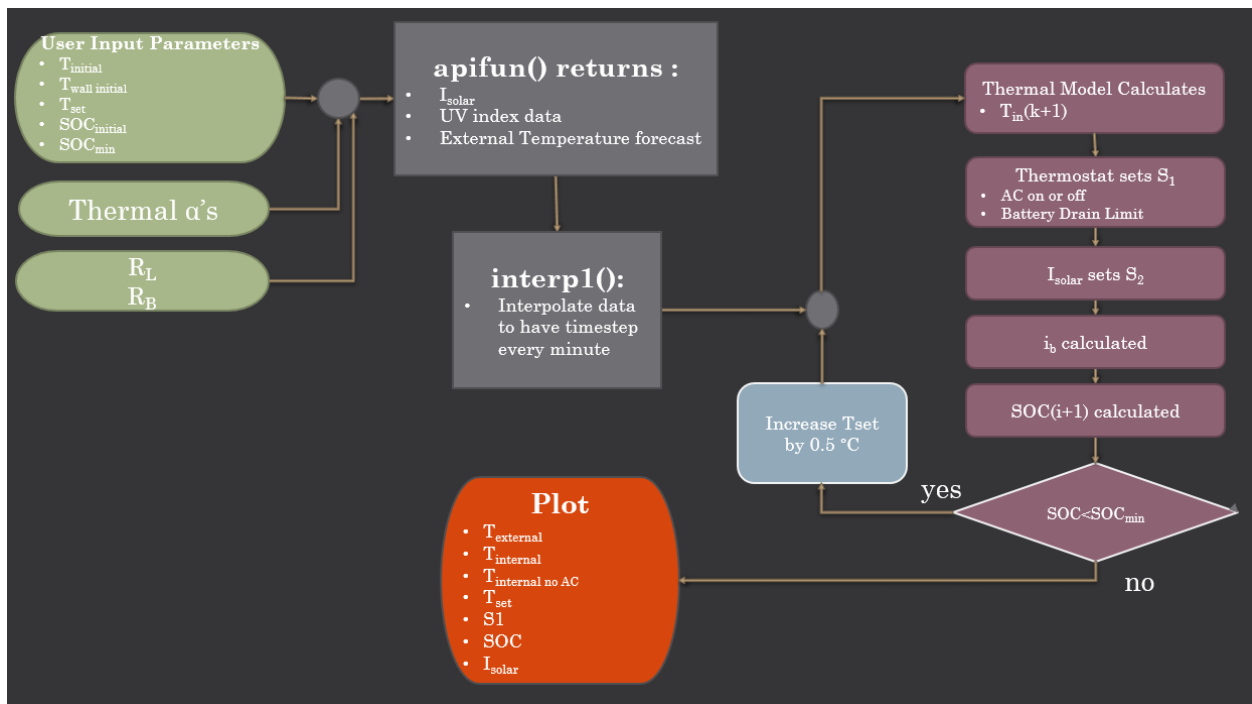


Figure 63) Matlab code flow chart

The user establishes the necessary input parameters while some parameters are preset such as the alpha coefficients and the resistances of the battery and air conditioner. A separate function was written to access forecast data from wunderground via an API. The function executes and returns forecasted current from the solar panels, UV index data and external temperature forecast. All for the next 60 hrs. Since this data is generated on an hourly basis or timestep the function interp1() is used to interpolate the data timestep to every minute. Data is then generated discretely for each time step in a for loop. First the internal temperature is calculated dictating whether the air conditioner needs to come on or not. The state of current from the solar panels is dependent on the  $I_{solar}$  values returned from the apifun().  $S_2$  is open if  $I_{solar}$  is greater than zero. Based on the switch scenario  $i_b$  (battery current) is calculated. The current conditions then dictate what the SOC at the end of the timestep will be therefore  $SOC(k+1)$  is

calculated. A SOC threshold was set by the user and it is verified that the SOC did not dip below this value for any of the timesteps. If it did the set point temperature will be increased by 0.5 degrees and the simulation run again until the battery is not drained past its SOC threshold value. The user has an ideal temperature that they would like however based on the battery power limitations the program offers a set point temperature that will not drain the battery past a user specified threshold.

### 3.2 Temperature Extremes

The external temperature forecasted from wunderground was offset by +25 C to demonstrate an extreme summer day. The desired internal temperature was set at 21 C. The plots below illustrate the intelligent aspect of the program.

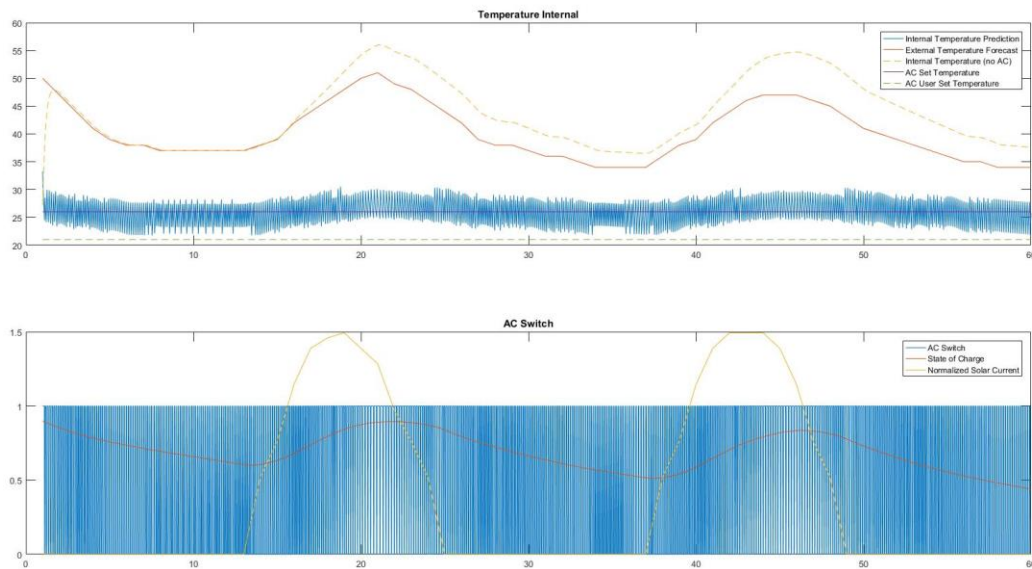


Figure 64) Intelligent temperature set point based on user restrictions

The 21 C set internal temperature was increased to 26 °C by the program because of the 40% SOC threshold placed on the system. With a setpoint temperature of 26 °C the battery will have a minimum discharge of 43% therefore meeting the criteria.

## 4.0 Conclusions and Future Work:

The first revision of the PCB board culminated with a skilled level of competence in Eagle software. Any future changes to components or footprints can be implemented relatively quickly. How to get a PCB manufactured was also a learning process from exporting the correct gerber files to coordinating with the vendor many lessons were learned along the way. Soldering of the board revealed lessons in surface mount soldering for various components. Mosfets, inductors, IC's, resistors, capacitors and many more were all soldered by hand requiring an extensive amount of patience. Although the execution of the PCB board was not in the final system many skills previously unknown were learned along the way.

Gathering data experimentally and applying it to construct a theoretical model was the back bone to the project. Hours learning new functions and techniques for MATLAB allowed the data to be processed successfully and implemented with a purpose.

Accessing data from a web server via an API was also a brand new undertaking and proved to be extremely powerful in the development of predictions. Instead of starting from ground zero the API allowed information to be access instantaneously, really relying on the work put forth by other developers. The project would not have been a success without there unsung effort.

The final model can be used to predict the ideal set point for the mobile residence but much work needs to be down to prove its accuracy. In the future the air conditioning unit will be installed on the van and a series of tests will be run to evaluate if the suggested temperature was actually maintained and whether the battery load stayed above the dictated threshold.

## References:

- [1] Bindzi Zogo Emmanuel Cedrick. “*Investment Motivation in Renewable Energy: A PPP Approach.*” *Alternative and Renewable Energy Quest.*
- [2] “*Reducing Energy Demand: A Review of Issues, Challenges and Approaches.*” *Reducing Energy Demand: A Review of Issues, Challenges and Approaches - ScienceDirect, Renewable and Sustainable Energy Reviews*, [www.sciencedirect.com/science/article/pii/S1364032115001471](http://www.sciencedirect.com/science/article/pii/S1364032115001471).
- [3] Ricardo Vidal Lorbada. “*Design and Implementation of a Charge Controller with Buck Converter Topology for a Li-Ion Battery Using the Component LTC4015.*” Dalarna University, European Solar Engineering School, 2016.
- [4] Cady, Stanton T., et al. “*Engineering Systems in the Re\_home: A Net-Zero, Solar-Powered House for the U.S. Department of Energy's 2011 Solar Decathlon.*” 2012 IEEE Power and Energy Conference at Illinois, 2012, doi:10.1109/peci.2012.6184583.
- [5] Dhople, Sairaj V., et al. “*Engineering Systems in the Gable Home: A Passive, Net-Zero, Solar-Powered House for the U. S. Department of Energy's 2009 Solar Decathlon.*” 2010 Power and Energy Conference At Illinois (PECI), 2010, doi:10.1109/peci.2010.5437154.
- [6] Lyn Bartram, Johnny Rodgers, and Kevin Muise. “*Chasing the Negawatt: Visualization for Sustainable Living.*” *IEEE Computer Graphics and Applications*, vol. 30, no. 3, 0ADAD, pp. 8–14., [ieeexplore.ieee.org/document/5455817/](http://ieeexplore.ieee.org/document/5455817/).
- [7] G. Wood and M. Newborough, “*Energy-Use Information Transfer for Intelligent Homes: Enabling Energy Conservation with Central and Local Displays,*” *Energy and Buildings*, vol. 39, no. 4, 2007, pp. 495–503.
- [8] Rohm. Capacitor Calculation for Buck Converter IC. [rohmfs.rohm.com/en/products/databook/applinote/ic/power/switching\\_regulator/capacitor\\_calculation\\_appli-e.pdf](http://rohmfs.rohm.com/en/products/databook/applinote/ic/power/switching_regulator/capacitor_calculation_appli-e.pdf).
- [9] Jason Arrigo. “*Input and Output Capacitor Selection.*” Application Report, Feb. 2006, [www.ti.com/lit/an/slta055/slta055.pdf](http://www.ti.com/lit/an/slta055/slta055.pdf).
- [10] Vieira, Filomeno M., et al. “*Energy Storage System for Self-Consumption of Photovoltaic Energy in Residential Zero Energy Buildings.*” *Renewable Energy*, vol. 103, 2017, pp. 308–320., doi:10.1016/j.renene.2016.11.048.
- [11] Xiao, Shunlong, et al. “*Model Predictive Control of Multi-String PV Systems with Battery Back-up in a Community Dc Microgrid.*” 2017 IEEE Applied Power Electronics Conference and Exposition (APEC), 2017, doi:10.1109/apec.2017.7930861.
- [12] Naoki Nitta, and Feixiang Wu. “*Li-Ion Battery Materials: Present and Future.*” *Materials Today*, vol. 18, no. 5, June 2015.

- [13] Linear Technologies. “*Multichemistry Buck Battery Charger Controller with Digital Telemetry System.*” [cds.linear.com/docs/en/datasheet/4015fb.pdf](https://cds.linear.com/docs/en/datasheet/4015fb.pdf).
- [14] Hart, Daniel W. *Power Electronics*. McGraw-Hill, 2011.
- [15] Erickson, Robert W., and Dragan Maksimovic. *Fundamentals of Power Electronics*. Kluwer Academic, 2001.
- [16] “*Enhancing Smart Grid with Microgrids: Challenges and Opportunities.*” Enhancing Smart Grid with Microgrids: Challenges and Opportunities - ScienceDirect, [www.sciencedirect.com/science/article/pii/S1364032117300746](http://www.sciencedirect.com/science/article/pii/S1364032117300746).
- [17] Hebatallah M. Ibrahim, et al. “*Dynamic Analysis of Buck-Based Photovoltaic Array Model.*” International Journal of Electrical Energy, Vol 1, no. No. 2, June 2013.
- [18] Mofakkarul Islam, and Md. Abul Bashar Sarkar. *An Efficient Smart Solar Charge Controller for Standalone Energy Systems - IEEE Xplore Document*, 2015 International Conference on Electrical Drives and Power Electronics, [ieeexplore.ieee.org/document/7325301](http://ieeexplore.ieee.org/document/7325301)
- [19] Chan, Korey, and Saeid Bashash. “Modeling and Energy Cost Optimization of Air Conditioning Loads in Smart Grid Environments.” *Volume 3: Vibration in Mechanical Systems; Modeling and Validation; Dynamic Systems and Control Education; Vibrations and Control of Systems; Modeling and Estimation for Vehicle Safety and Integrity; Modeling and Control of IC Engines and Aftertreatment Systems; Unmanned Aerial Vehicles (UAVs) and Their Applications; Dynamics and Control of Renewable Energy Systems; Energy Harvesting; Control of Smart Buildings and Microgrids; Energy Systems*, Nov. 2017, doi:10.1115/dscc2017-5284.
- [20] Canadian Solar. “Installation Manual of Standard Solar Modules (IEC).” [Canadiansolar.com](http://Canadiansolar.com).
- [21] Horowitz, Paul, and Winfield Hill. *The Art of Electronics*. Cambridge University Press, 1989.
- [22] “A WEATHER API DESIGNED FOR DEVELOPERS.” *Weather Underground (10.226.237.35)*, [www.wunderground.com/weather/api/](http://www.wunderground.com/weather/api/).

## Appendix A. Matlab Code:

```
clear
clc
close all

%User Inputs
Tin(1)=35;
Tw(1)=26;
Tset=21;
SOC(1)=.9;
SOCmax=.98;
SOCmin=.4;
Tinnoac(1)=25;
Twnoac(1)=28;
shaded=1;

%Prediction Data Functionf
```

```

[Isolar,UV,Tforecast]=apifun();

%Isolar shaded degredation
Isolar = Isolar.*shaded;

%1 minute timestep adjustment
timemin=(1:(60/3660):60);
timehour=(1:1:60);
Isolarmin=interp1(timehour,Isolar,timemin);
UVmin=interp1(timehour,UV,timemin);
tempout=interp1(timehour,Tforecast,timemin);
Isolarmin=Isolarmin';
UVmin=UVmin';
tempout=tempout';
timestep=timemin;
Tsetuser=(Tset*ones(1,3600))';

% Second Order Thermal Model
x = [.00015 .0842 .0018 -.0204 .0214 1.56 3];
alphaw1 = x(1);
alphaa1 = x(2);
alphasun1 = x(3);
alphaw2 = x(4);
alphaaw = x(5);
alphasun2 = x(6);
alphaac = x(7);
timestep=1;
Tdb=.5;
ac(1)=1;

%Electrical Parameters
RL=.311;
RB=.3;

for j=1:20

for i=1:3600
    Tin(i+1) = Tin(i)+(timestep*((Tin(i)*(-alphaw1-
alphaa1)))+(alphaw1*Tw(i)))+(alphaa1*tempout(i))+(alphasun1*UVmin(i))-
(alphaac*ac(i)));
    Tw(i+1) = Tw(i)+(timestep*((Tw(i)*(-alphaw2-
alphaaw)))+(alphaw2*Tin(i)))+(alphaaw*tempout(i))+(alphasun2*UVmin(i)));

    Tinnoac(i+1) = Tinnoac(i)+(timestep*((Tinnoac(i)*(-alphaw1-
alphaa1)))+(alphaw1*Twnoac(i)))+(alphaa1*tempout(i))+(alphasun1*UVmin(i)));
    Twnoac(i+1) = Twnoac(i)+(timestep*((Twnoac(i)*(-alphaw2-
alphaaw)))+(alphaw2*Tinnoac(i)))+(alphaaw*tempout(i))+(alphasun2*UVmin(i)));

%Thermostat
if Tin(i)>=Tset+Tdb
    s1(i)=1;
    ac(i+1)=1;

```

```

else if Tin(i) <= Tset-Tdb
    s1(i)=0;
    ac(i+1)=0;
    else
        s1(i)=s1(i-1);
        ac(i+1)=ac(i);
    end
end

%Switch 2 Logic
if Isolarmin(i) >= .01
    s2(i)=1;
end
if Isolarmin(i) == 0
    s2(i)=0;
end
if SOC(i) >= SOCmax
    s2(i)=0;
end

%Battery Drain Limit
if SOC(i) < SOCmin;
    s1(i)=0;
    iload(i)=0;
else
    iload(i)=3;
end

%Switch Scenarios
if s1(i)==1 && s2(i)==1
    ib(i) = (((15/9)*SOC(i))+12.833) - ((RL*Isolarmin(i))) / (RB+RL);

else if s1(i)==1 && s2(i)==0
    ib(i) = ((15/9)*SOC(i))+12.833 / (RB+RL);

else if s1(i)==0 && s2(i)==1
    ib(i) = -Isolarmin(i);

else if s1(i)==0 && s2(i)==0
    ib(i)=0;
end
end
end

%State of Charge
SOC(i+1)=SOC(i) - ((1/(260*3600))*60*ib(i)) + ((1/(260*3600))*60*iload(i));

```

```

end
    Tsetlimit(j)= Tset+.5;
    %Tsetlimit=(Tset:.5:Tset+10)';
    Batlow=min(SOC);
    if Batlow<=SOCmin;
        Tset=Tsetlimit(j);
    else
        break
    end
end

end

Tin = Tin';
Tw = Tw';
Tset = Tset*ones(1,3600);

figure
subplot(2,1,1)
plot(timemin,Tin(2:end));
title('Temperature Internal')
hold on
plot(timemin,tempout);
plot(timemin,Tinnoac(2:end),'--');
plot(timemin,Tset);
plot(timemin,Tsetuser,'--');
legend('Internal Temperature Prediction','External Temperature
Forecast','Internal Temperature (no AC)','AC Set Temperature','AC User Set
Temperature');
hold off

subplot(2,1,2)
plot(timemin,s1);
title('AC Switch')
hold on
plot(timemin,SOC(1:end-1));
plot(timemin,(Isolarmin./25));
legend('AC Switch','State of Charge','Normalized Solar Current');
hold off

```

## Appendix B. API Matlab Code:

```

function
[Isolar,UV,Tforecast]=apifun(alphaw1,alphaa1,alphasun1,alphaw2,alphaaw,alphas
un2,alphaac)

%%API Wunderground
key = '22d6314cfd649ff8';
options = weboptions('ContentType','json');

CallURL_forecast =
['http://api.wunderground.com/api/22d6314cfd649ff8/hourly10day/q/CA/Morgan_Hi
ll.json'];
Forecast_Data = webread(CallURL_forecast, options);

```

```

disp('Forecast');

tempstruct = cat(1,Forecast_Data.hourly_forecast.temp);
CompleteTforecast = str2double({tempstruct.metric}');
Tforecast = CompleteTforecast(1:60)+25;
time = (0:1:(length(Tforecast)-1))';

Condition = {Forecast_Data.hourly_forecast.condition}';
UV1 = str2double({Forecast_Data.hourly_forecast.uvi}');
UV = UV1(1:60);

scaling = ones(size(Condition));

%% Lookup table example (with logical indexing)
lookup = {'Light Drizzle',      0.5;
          'Heavy Drizzle',     0.5;
          'Drizzle',           0.5;
          'Light Rain',        0.5;
          'Heavy Rain',        0.5;
          'Rain',              0.5;
          'Light Snow',        0.5;
          'Heavy Snow',        0.5;
          'Snow',              0.5;
          'Light Snow Grains', 0.5;
          'Heavy Snow Grains', 0.5;
          'Snow Grains',       0.5;
          'Light Ice Crystals',0.5;
          'Heavy Ice Crystals',0.5;
          'Ice Crystals',      0.5;
          'Light Ice Pellets', 0.5;
          'Heavy Ice Pellets', 0.5;
          'Ice Pellets',       0.5;
          'Light Hail',        0.5;
          'Heavy Hail',        0.5;
          'Hail',              0.5;
          'Light Mist',        0.5;
          'Heavy Mist',        0.5;
          'Mist',              0.5;
          'Light Fog',         0.5;
          'Heavy Fog',         0.5;
          'Fog',               0.5;
          'Light Haze',        0.5;
          'Heavy Haze',        0.5;
          'Haze',              0.5;
          'Light Rain Mist',   0.5;
          'Heavy Rain Mist',   0.5;
          'Rain Mist',         0.5;
          'Light Rain Showers',0.5;
          'Heavy Rain Showers',0.5;
          'Rain Showers',      0.5;
          'Light Thunderstorm',0.5;
          'Heavy Thunderstorm',0.5;
          'Thunderstorm',      0.5;
          'Light Thunderstorm and Rain',0.5;
          'Heavy Thunderstorm and Rain',0.5;

```

```

        'Thunderstorm and Rain',      0.5;
        'Light Thunderstorm and Snow',0.5;
        'Heavy Thunderstorm and Snow',0.5;
        'Thunderstorm and Snow',     0.5;
        'Patches of Fog',            0.5;
        'Shallow Fog',               0.5;
        'Overcast',                  0.5;
        'Clear',                     0.5;
        'Partly Cloudy',             0.5;
        'Mostly Cloudy',             0.5;
        'Scattered Clouds',         0.5;
        'Small Hail',                0.5;
        'Unknown',                   0.5;
        'Chance of Rain',            0.5;});

for ii = 1:length(lookup)
    logic = strcmp(Condition,lookup{ii,1});
    scaling(logic) = lookup{ii,2};
end

%% Thermal Model
x = [.00015 .0842 .0018 -.0204 .0214 1.56 3];
alphaw1 = x(1);
alphaa1 = x(2);
alphasun1 = x(3);
alphaw2 = x(4);
alphaaaw = x(5);
alphasun2 = x(6);
alphaaac = x(7);
timestep=1;
Tin(1)=20;
Tw(1)=20;
ac=0;
%
% for i=1:(length(Tforecast)-1)
%     Tin(i+1) = Tin(i)+(timestep*((Tin(i)*(-alphaw1-
alphaa1)))+(alphaw1*Tw(i)))+(alphaa1*CompleteTforecast(i)))+(alphasun1*UV(i))+(a
lphaaac*ac));
%     Tw(i+1) = Tw(i)+(timestep*((Tw(i)*(-alphaw2-
alphaaaw)))+(alphaw2*Tin(i)))+(alphaaaw*CompleteTforecast(i)))+(alphasun2*UV(i))
;
% end
% Tin = Tin';
% Tw = Tw';
%
% time = (1:1:length(Tforecast))';
%
% plot(time,Tin,'r','LineWidth',2);
% hold on
% plot(time,Tforecast,'g','LineWidth',2);
% xlabel('Time [Hr]');
% ylabel('Temperature [C]');
% legend('Internal Temperature Model','Wunderground External Temperature');

%% Solar Current
for i=1:(length(Tforecast))

```

```
if UV(i) > 0
    Isolar(i) = ((-11.028*(UV(i)^2)) + (187.62*UV(i)) + 153.017) / 25.4;
else
    Isolar(i) = 0;
end
```

```
end
```

```
Isolar = Isolar';
%plot(time, Isolar);
```